Published in final edited form as:

*J Med Chem*. 2002 September 26; 45(20): 4471–4484. doi:10.1021/jm020211+.

# Structural Determinants of $A_3$ Adenosine Receptor Activation: Nucleoside Ligands at the Agonist/Antagonist Boundary

**Zhan-Guo Gao**[‡], **Soo-Kyung Kim**[‡], **Thibaud Biadatti**[†], **Wangzhong Chen**[‡], **Kyeong Lee**[‡], **Dov Barak**[§], **Seong Gon Kim**[‡], **Carl R. Johnson**[†], **Kenneth A. Jacobson**[*,‡]

[‡]Molecular Recognition Section, Laboratory of Bioorganic Chemistry, National Institute of Diabetes and Digestive and Kidney Diseases, National Institutes of Health, Bethesda, Maryland 20892

[†]Department of Chemistry, Wayne State University, Detroit, Michigan 48202-3489

[§]Israel Institute for Biological Research, Ness Ziona, Israel

## Abstract

Mutagenesis of the human $A_3$ adenosine receptor (AR) suggested that certain amino acid residues contributed differently to ligand binding and activation processes. Here we demonstrated that various adenosine modifications, including adenine substitution and ribose ring constraints, also contributed differentially to these processes. The ligand effects on cyclic AMP production in intact CHO cells expressing the $A_3$AR and in receptor binding were compared. Notably, the simple 2-fluoro group alone or 2-chloro in combination with $N^6$-substitution dramatically diminished the efficacy of adenosine derivatives, even converting agonist into antagonist. Other affinity-increasing substitutions, including $N^6$-(3-iodobenzyl) **4** and the (Northern)-methanocarba **15**, also reduced efficacy, except in combination with a flexible 5′-uronamide. 2-Cl-$N^6$-(3-iodobenzyl) derivatives, both in the (*N*)-methanocarba (i.e., of the Northern conformation) and riboside series **18** and **5**, respectively, were potent antagonists with little residual agonism. Ring-constrained 2′,3′-epoxide derivatives in both riboside and (*N*)-methanocarba series **13** and **21**, respectively, and a cyclized (spiral) 4′,5′-uronamide derivative **14** were synthesized and found to be human $A_3$AR antagonists. **14** bound potently at both human (26 nM) and rat (49 nM) $A_3$ARs. A rhodopsin-based $A_3$AR model, containing all domains except the C-terminal region, indicated separate structural requirements for receptor binding and activation for these adenosine analogues. Ligand docking, taking into account binding of selected derivatives at mutant $A_3$ARs, featured interactions of TM3 (His95) with the adenine moiety and TMs 6 and 7 with the ribose 5′-region. The 5′-OH group of antagonist $N^6$-(3-iodobenzyl)-2-chloroadenosine **5** formed a H-bond with N274 but not with S271. The 5′-substituent of nucleoside antagonists moved toward TM7 and away from TM6. The conserved Trp243 (6.48) side chain, involved in recognition of the classical (nonnucleoside) $A_3$AR antagonists but not adenosine-derived ligands, displayed a characteristic movement exclusively upon docking of agonists. Thus, $A_3$AR activation appeared to require flexibility at the 5′- and

[*]Corresponding author: Dr. K. A. Jacobson, Chief, Molecular Recognition Section, Bldg. 8A, Rm. B1A-19, NIH, NIDDK, LBC, Bethesda, MD 20892-0810. Tel: 301-496-9024; fax: 301-480-8422; kajacobs@helix.nih.gov.

**Supporting Information Available:** Synthetic methods for preparation of compounds **25**–**35** and **14**. This material is available free of charge via the Internet at http://pubs.acs.org.

3′-positions, which was diminished in (*N*)-methanocarba, spiro, and epoxide analogues, and was characteristic of ribose interactions at TM6 and TM7.

## Introduction

The structure–activity relationship (SAR) of nucleosides acting as agonists at adenosine receptors (ARs) has been studied mainly at the "classical" $A_1$ and $A_{2A}$AR subtypes. Several review articles[1,2] have summarized known SAR of adenosine derivatives, based primarily on radioligand binding experiments. Modifications of nucleosides (Chart 1) known to increase receptor binding affinity among adenosine agonists include: 5′-uronamides such as **1**, substitutions at the 2- (**2**, **3**) and $N^6$-positions (**4–7**), or the replacement of the adenine moiety with a 1,3-substituted xanthine moiety (**8**). A pair of $N^6$-phenylisoproyl *R*- and *S*-diastereomers **9** and **10** has demonstrated stereoselectivity of binding at $A_1$ and $A_{2A}$ARs.[3] Combinations of these groups, as in the $A_3$AR-selective agonists **11** and **12**, are often additive in their potency enhancement.[4] Such modifications also enhance the stability of adenosine derivatives in biological systems, principally by preventing the action of adenosine deaminase at the 6-position and/or adenosine kinase at the 5′-position. The ribose moiety has also been replaced effectively with a ring-constrained (*N*)-methanocarba group (Chart 2),[5,6] which selects a conformation that favors binding at the $A_3$AR versus the other subtypes. Thus, (*N*)-methanocarba derivatives **16**, **19**, and **20**, which also contain a 5′-uronamide group, were shown to be potent and selective full agonists at the $A_3$AR.

Several studies[7–9] have suggested that modification of the adenosine structure may reduce efficacy at one or more of the AR subtypes. For example, C-8 substitution was shown to reduce efficacy of **6** at the $A_1$AR.[8] C-2 substitution was shown to reduce efficacy of adenosine derivatives acting at the $A_3$AR.[8,9] We recently reported the unexpected result that the commonly used $A_1$AR-selective agonist **7** acted as an antagonist at the human $A_3$AR,[9] and this theme is expanded in the present study. These findings suggest that rational modification of adenosine agonists into antagonists may be possible. There are many nonnucleoside classes of $A_3$AR receptor antagonists;[1,10] however, the approach of converting adenosine derivatives into pure antagonists of high affinity has not previously succeeded.[11] Moreover, antagonists of high affinity and selectivity at nonprimate species are still lacking.[9,10] This study may remedy that lack, since the lead compounds, i.e., adenosine agonists, are typically of high affinity across species.[12] For other G protein-coupled receptors, there are examples of minor modifications in the structure of agonists leading to loss of efficacy, e.g., conversion of agonists to antagonists at $P2Y_1$ nucleotide receptors,[13] opiate receptors,[14] and neurokinin receptors.[15]

In this study, we compared binding and functional properties of representative ligand probes, i.e., both previously reported[2,4–6] and novel derivatives of adenosine. To probe the effects of rigidifying the ribose moiety, novel 2′-,3′-epoxide derivatives **13** and **21**, in both riboside and (*N*)-methanocarba series, respectively, and a cyclized (spiro) 4′,5′-uronamide derivative **14** were prepared. We have categorized modifications of adenosine, including adenine substitution and ribose ring constraints, according to their typically differential effects on the binding and activation processes at the $A_3$AR, and explained the results based on a

receptor model. The proposed mode of docking nucleoside-based agonists and antagonists the $A_3$AR also took into account binding characteristics of selected derivatives at mutant $A_3$ARs.

## Results

### Chemical Synthesis.

The 2′,3′-anhydroadenosine derivative **21** was synthesized as shown in Scheme 1. The (*N*)-methanocarba triol **18** was treated with α-acetoxyisobutyryl bromide in wet acetonitrile,[16,17] followed by direct treatment of the mixture of both isomers of *trans*-3′(2′)-bromo-2′(3′)-acetate with Amberlite ($OH^-$) resin in methanol.[18] Similarly for the 5′-methylamide **12** epoxidation at the 2′,3′-positions was accomplished by reaction with α-acetoxyisobutyryl bromide followed by cyclization in base to yield **13**.

The spiral analogue **14** was synthesized in 10 steps (Scheme 2) from a brominated cyclopentenone derivative **24**. The use of enantiopure **24** in the synthesis of 4-methyl ribose systems has been described.[19,20] For the synthesis of the target molecule **14**, a more functionalized side chain has to be incorporated into the ribose system. Allylmagnesium bromide was added to **24** providing the acid labile tertiary alcohol **25**. Direct ozonolysis of **25** in methanol/pyridine led to ribose derivative **27** but only in modest yield and on a small scale and was unsuccessful when attempted on a larger scale. Protection of the external alkene as the dibromide followed by ozonolysis afforded the ribose framework **28** in 82% yield. Conversion of **28** to the β-methylglycoside **29** and reductive elimination of bromine smoothly provided the 4-allylribose **30**. Ozonolysis of **30** followed by reductive amination with 4-methyoxybenzylamine/$NaBH_3CN$ gave lactam **31**. Oxidation of **31** with ceric ammonium nitrate gave a mixture of deprotected **32** and the benzoyl derivative **33**. The latter was readily converted to **32** upon treatment with potassium carbonate in methanol. To proceed with Vorbrüggen nucleosidation,[21] the isopropylidene protection was exchanged for acetate by treatment of **32** with HCl in methanol. Treatment of **34** with silylated 6-chloropurine and TMS triflate in acetonitrile at 65 °C followed by chromatography of the product mixture gave nucleoside **35** in 81% yield. Brief exposure of **35** to ammonia and then 3-iodobenzylamine gave the target **14** in 87% yield.

### Biological Activity.

**(a) Interaction of a Wide Range of Adenosine Derivatives with the Human $A_3$AR Stably Expressed in CHO Cells.—**The binding and activation of the human $A_3$AR by a wide range of adenosine derivatives (Charts 1 and 2) were investigated. Binding was studied using the radioiodinated form of the agonist $N^6$-(4-amino-3-iodobenzyl)adenosine-5′-*N*-methyluronamide ([$^{125}$I]**36**),[22] and functional effects on forskolin-stimulated cyclic AMP production were examined in intact Chinese hamster ovary (CHO) cells expressing the human $A_3$AR (Table 1).[23] The previously reported adenosine derivatives[1] used in this study include the $A_1$AR selective agonists **6**, **7**, **9**, and **10**; an $A_{2A}$ receptor selective agonist 2-[*p*-(carboxyethyl)phenylethylamino]-5′-*N*-ethylcarboxamidoadenosine **37**; the $A_3$ selective ligands **4**, **5**, **11**, **12**, **16**, **17**, **18**, **19**, and **20**; the ligands of low selectivity **1**, **2**, **3**, **8**, **15**, and **36**; and the newly synthesized

derivatives **13**, **14**, and **21**. Some of these adenosine derivatives, including $N^6$-(3-iodobenzyl) derivatives **11** and **12**, already demonstrated to be potent $A_3$AR agonists,[2,4–6] were included as reference compounds in the present study. Other adenosine derivatives, especially those newly synthesized, had not previously been evaluated in functional assays, and might otherwise be presumed to be agonists being adenosine derivatives.

In the derivatives $A_3$AR binding assay, the 2-chloro substituent and the $N^6$-iodobenzyl group generally increased the affinity of the adenosine, while the substitution of the ribose moiety with an (*N*)-methanocarba moiety[5,6] slightly decreased or did not influence the affinity significantly.

A recent report[9] demonstrated that the potent $A_1$AR agonist $N^6$-cyclopentyladenosine **6** is also a full agonist at $A_3$ARs, while the corresponding 2-chloro derivative **7** is a moderately potent, full antagonist at the $A_3$AR. However, it was not clear if other 2-chloro-substituted analogues would behave like **6** or like **7**. To explore further the effects of the 2-chloro substituent in the activation of the human $A_3$AR, two pairs of $N^6$-(3-iodobenzyl) adenosine derivatives with or without chloro substituent (the ribosides **4** versus **5** and the methanocarba derivatives **17** versus **18**) were compared. Figure 1 demonstrated that **4** was more efficacious than **5**, while **17** was more efficacious than **18**. 5′-Alcohol derivatives **5** and **18** and the spiral derivative **14** were demonstrated to have little if any detectable agonist activity (Table 1), suggesting possible antagonism. This was further demonstrated by their effects on the concentration–response curve of the agonist-induced inhibition of forskolin-stimulated cyclic AMP production in intact CHO cells (Figure 2). They shifted the agonist concentration–response curve to the right in a dose-dependent manner, corresponding to $K_B$ values[24] of 2.4 ± 0.4, 3.0 ± 0.6, and 2.0 ± 0.3 nM for compounds **5**, **14** (not shown), and **18**, respectively.

The observation that **17** was less efficacious than **4** (Figure 1) suggested that the replacement of the ribose ring by an (*N*)-methanocarba ring system may also decrease agonist efficacy. Hence, we further compared another pair of compounds, the 2-chloro riboside **3** and the corresponding (*N*)-methanocarba derivative **15**. Compound **3** was a full agonist at the human $A_3$AR, while **15** was a partial agonist (Figure 3A) with a maximal efficacy of ~40% of the maximal efficacy of **3**.

The 2-chloro substituent decreased the agonist efficacy for a number of multi-substituted adenosine analogues; however, this was not a general phenomenon, since the 2-chloro substituted **12**, and **20**, and 2-chloroadenosine **3** itself, were full agonists at the human $A_3$AR. Hence, the efficacy-diminishing effect of the chloro substituent also depended on which additional structural features such as an $N^6$-substituent were present. Curiously, the smaller and more polar 2-fluoro substituent (see **2**) was able to decrease the efficacy as $A_3$AR agonist, even in an absence of $N^6$-substituent. Compound **2** proved to be a partial agonist at the $A_3$AR, with ~30% of the maximal efficacy of **3** (Table 1).

It has been suggested that the ribose 2′ and 3′-hydroxyl groups are critical in the activation of $A_1$ARs.[25,26] Here we further examined the role of these two hydroxy groups in the activation of $A_3$ARs. The epoxidation of the two hydroxyl groups of the potent agonist **12**

resulting in compound **13** led to a decrease of binding affinity by more than 1000-fold, and the efficacy was also dramatically decreased to only ~7% the maximal efficacy of **12** (Figure 3B). Similarly, the epoxidation of the methanocarba derivative **18** resulting in compound **21** also induced a 300-fold affinity decrease, suggesting the critical role of one or both of the hydroxyl groups in binding and activation processes at the human $A_3$AR.

To further analyze the structural determinants of activation of the human $A_3$AR, we tested compound **8**, a 5′-uronamide derivative in which the adenine moiety was replaced with a 1,3-dibutylxanthine moiety. Although the 1,3-dialkylxanthine moiety alone is an AR antagonist, **8** was found to be a full agonist at the human $A_3$AR (Figure 3B), similar to previous findings with the rat $A_3$AR.[12] It should also be noted that 1,3-dibutylxanthine itself has extremely low affinity for the $A_3$AR, and the ribose attachment increased both the affinity and the efficacy of the xanthine derivative (data not shown).

**(b) Effects of a Nucleotide GTPγS on the Displacement of an Antagonist Radioligand by the Adenosine Derivatives.—**The effects of some of the adenosine derivatives on the human $A_3$AR were further examined utilizing a functional assay based on the method of guanine nucleotide-induced shift of agonist competing for antagonist radioligand binding.[8,22,27] [$^3$H]8-ethyl-4-methyl-2-phenyl-(8*R*)-4,5,7,8-tetrahydro-1H-imidazo[2,1-i]-purin-5-one is a novel $A_3$AR-selective radioligand introduced by Müller et al.[28] and has recently been used to characterize the human $A_3$AR.[23,29] The nonhydrolyzable GTP analogue, GTPγS (100 μM), caused a 4-fold decrease in the affinity of the agonist **12** in competition for [$^3$H]8-ethyl-4-methyl-2-phenyl-(8*R*)-4,5,7,8-tetrahydro-1H-imidazo[2,1-i]-purin-5-one binding (Table 2), but it only had a slight or no effect on the affinity of adenosine-derived antagonists **5**, **7**, **14**, and **18**. This indicated that in this functional assay these four nucleosides behaved essentially the same as the classical $A_3$AR antagonist **38** *N*-[9-chloro-2-(2-furanyl)-[1,2,4]triazolo[1,5-c]quinazolin-5-yl]benzene-aceta-mide.[9,22] Thus, the unexpected loss of agonism among various adenosine derivatives was confirmed using several different methods[5] of determining the degree of receptor activation.

**(c) Modulation of the Binding of Adenosine Derivatives to the Human $A_3$AR by H95A and W243A Mutations.—**We further[29] examined the binding of a number of adenosine derivatives with or without a 2-chloro substituent to the wild type and H95A mutant ARs (Table 3). The H95A mutation induced a larger rightward shift of the compounds having a 2-chloro substituent, although the range of shift also depended on additional substitution. Indeed, although a fairly subtle change in structure, addition of a 2-chloro substituent had a major effect on the interaction of adenosine derivatives with the $A_3$AR.

A tryptophan residue (W243) in TM6 has been suggested to be involved in antagonist binding to the human $A_3$AR.[29] Here we further examined the interactions of the present set of adenosine derivatives with wild type and W243A mutant receptors (Table 3). It was found that this residue was involved in the binding of only nonnucleoside antagonists such as 5-propyl-2-ethyl-4-propyl-3-(ethylsulfanylcarbonyl)-6-phenylpyridine-5-carboxylate **39** and the S-enantiomer of 1,4-dihydro-2-methyl-6-phenyl-4-

(phenylethynyl)-3,5-pyridinedicarboxylic acid, 3-ethyl 5-(phenylmethyl) ester **40**. However, mutation of this residue had no effect on the affinity of either agonists or antagonists derived from adenosine (Figure 4). Hence, this residue discriminated antagonist ligands of different chemical classes.

**(d) Effects of the Adenosine Derivatives on Rat ARs.—**It is known that currently available $A_3$AR antagonists, including **38**[22] and 5-[[(4-methoxyphenyl)amino]-carbonyl]amino-8-propyl-2-(2-furyl)-pyrazolo[4,3-e]1,2,4-triazolo[1,5-c]pyrimidine (MRE 3008F20),[30] have very high affinity for the human $A_3$AR, but low affinity for the rat $A_3$AR. In contrast, typical $A_3$AR agonists have similar $A_3$AR affinity in both species. Hence, potent rat $A_3$AR antagonists could be identified by modifying the structure of the adenosine and adenosine derivatives. As shown in Table 4, antagonists **5** and **18** displayed high affinity for both the recombinant rat $A_3$AR transfected in CHO cells and the endogenous rat $A_3$AR in RBL-2H3 basophils.[12] The potent human $A_3$AR triazoloquinazoline antagonist[22] **38** at 10 $\mu$M displaced less than 50% of [$^{125}$I]**36** binding. Consistent with lack of agonism neither **5** nor **18** at ≤ 10 $\mu$M induced a significant inhibition of forskolin-stimulated cyclic AMP production in CHO cells expressing the rat $A_3$AR (data not shown).

The $K_i$ values (nM) at rat brain ARs were measured as described.[6] The $K_i$ values ($\mu$M) were determined to be 3.92 ± 0.40 ($A_1$) and >20 ($A_{2A}$) for **13**, 12.1 ± 2.4 ($A_1$) and 20.8 ± 0.4 ($A_{2A}$) for **14**, and 24.2 ± 3.8 ($A_1$) and 47.9 ± 7.0 ($A_{2A}$) for **21**.

**(e) Molecular Modeling of the Human $A_3$AR and Ligand Docking.—**3D-structures of all domains of the $A_3$AR except the C-terminal region were newly constructed using homology modeling from the X-ray structure of rhodopsin.[31] The inclusion of loop regions reduced the large deviation of the end of the TM bundles, since the previous $A_3$AR model[32] had a high rmsd (root-mean-squared deviation) value between backbone atoms in the α-helix relative to the rhodopsin structure. To validate the reliability of the calculated model, stereochemical accuracy, packing quality, and folding reliability were checked. Using a Ramachandran plot, $\varphi$ and $\psi$ angles were compared with the rhodopsin crystal structure. All amino acids in the α-helices were located in the favored region of right-handed α-helix in the Ramachandran plot. Only 3% of the residues within loop segments were in the sterically disallowed region. From calculated $\omega$ angles, there were no cis peptide bonds in the calculated $A_3$AR model as well as in the rhodopsin structure. All $C_\alpha$ atoms except Cys displayed S-chirality. For the packing quality, there were no bump regions in the calculated $A_3$AR model. To check the folding reliability, the rmsd between backbone atoms in α-helix of the calculated $A_3$AR model and the template molecule was found to be 1.37 Å, compared to 2.69 Å in the previous model.[32] Both structures showed overall similarities, especially the regions having defined secondary structures.

We used an automated docking procedure to determine the most favorable binding locations and orientations for several ligands (**1**, **4**, **5**, **12**, and **14**) and compared these results with our experimental results. An energetically favorable model that correlated well with the experimental result was selected.

The putative binding site surrounding the full agonist **12** docked in the $A_3$AR is shown in Figure 5A. Residues that were within 5 Å proximity to the ligand in this putative binding site were: L91 (3.33), T94 (3.36), H95(3.37), Q167 (EL2), F168 (EL2), F182 (5.43), F239 (6,44), W243 (6.48), L246 (6.51), N250 (6.55), S271 (7.42), H272 (7.43), and N274 (7.45). Mutagenesis results for several AR subtypes[29,33–35] were consistent with molecular modeling that featured direct interaction of ligands with TMs 3, 6, 7, and EL2.

The purine ring was located in a hydrophobic pocket defined by L91 (3.33) and H95 (3.37) and the amine of the $N^6$-substituent interacted with N250 (6.55) through H-bonding, which was similar to our $A_{2A}$AR docking model.[33] The inability of the N250A mutant $A_3$AR[29] or the corresponding mutant $A_{2A}$AR[33] to bind either radiolabeled agonist or antagonist was consistent with a proposed direct interaction of this residue with **12** and other ligands. Additional aromatic-aromatic stabilization of the $N^6$-benzyl group in compound **12** interacting with surrounding F182 (5.43) and F168 (EL2) may be responsible for the increase of binding affinity. The 2′-OH and 3′-OH groups of the ribose ring were involved in H-bonding with Q167 (EL2) and H272 (7.43), respectively, which was supported by our $A_3$AR neoceptor model.[32] The epoxidation of 2′- and 3′-OH groups decreased the binding affinity by about 1000-fold (compound **12** vs **13**) supporting a possible direct interaction of the hydroxyl group(s) with the receptor. The carbonyl and amino groups of the 5′-uronamide substituent of **12** formed H-bonds with S271 (7.42) and T94 (3.36). An additional hydrophobic interaction between the terminal alkyl group at the 5′-position and F239 (6.44) stabilized the complex.

A difference in comparison to our former model[29] was seen in the role of H95. Our previous human $A_3$AR model[29] featured a direct interaction between the 2-chloro substituent of adenosine derivatives with a histidine residue (H95) in the third transmembrane domain (TM3) of the human $A_3$AR, yet experimental evidence did not support such an interaction.[29] The present study demonstrated the role of the 2-chloro substituent in ligand recognition by the human $A_3$AR, yet it did not postulate a direct contact with H95, thus removing the discrepancy. The previous model[29] proposed a conformation about the glycosidic bond that was intermediate between syn- and anti-conformations and also a direct interaction of the 2-Cl substituent with the side chain of H95. However, the relative energy difference between the intermediate and anti-conformations of the purine ring of **12** and other ligands in bound complex showed that the anti-conformation, which did not show a direct interaction with the H95 side chain, was more energetically favorable than the intermediate conformation in the $A_3$AR. In the anti-conformation, H95 was a component of the hydrophobic pocket that accommodated the purine ring through hydrophobic interaction. This model featuring the anti-conformation as active conformation of full agonists **1** and **12** was consistent with the binding studies of methanocarba-adenosine analogues,[5,6] since the (*N*)-methanocarba modification of adenosine stabilized the anti-conformation.[6] The other evidence which did not support a direct 2-Cl–H95 interaction was that the H95A mutation reduced the binding affinity of both 2-Cl and 2-H adenosine analogues, although the effect on 2-Cl-analogues was larger. Cl may be involved indirectly by altering the hydrophobic interaction with the purine ring by inducing a change of $\pi$-electron density due to its electron-withdrawing

effect. The efficacy-reducing effect of 2-F would be consistent with an electronic effect of 2-substitution.

Binding modes of nucleoside 5′-*N*-alkyluronamide-containing agonists **1** and **12** compared to nucleoside antagonists **5** and **14** were different with respect to the 5′-position of the ribose ring. The association with TMs 6 and 7 with the flexible alkylamide group of 5′-uronamide agonists **1** and **12** was stabilized by hydrophobic interaction with F239 (6.44) as well as by H-bonding with S271 (7.42) and T94 (3.36). In the case of nucleoside antagonist binding, the 5′-OH group of $N^6$-(3-iodobenzyl)-2-chloroadenosine **5** formed a H-bond with N274 but not with S271. This bonding occurred as a result of a small movement of the 5′-substituent toward TM7 and away from TM6. The carbonyl group of the cyclic amide in the antagonist **14** still retained H-bonding with S271 (7.42) but lost additional H-bonding with T94 (3.36) due to the different geometry of NH in flexible versus rigid alkylamide groups.

Another pronounced difference between nucleoside agonist 5′-*N*-alkyluronamide derivatives **1** and **12** and the antagonists **5** and **14** seen in the docked $A_3$AR complexes was the position of the conserved W243 (6.48). For antagonists **5** or **14** the model achieved energetic convergence without the movement of the side chain of W (Figure 5B,C), while the model with full agonist **12** (Figure 5A) could not optimize until the W side chain was moved within the binding pocket. The interaction between the W side chain and the 5′-alkyl group was sterically unfavorable. The comparison of the positions of side chains surrounding the putative binding site of **12** before versus after docking shows that only W243 underwent substantial movement (Figure 6). This movement, which was required for binding of the two above-mentioned agonist nucleosides, may be one of the components in the overall conformational change of ARs induced by agonist binding. In the absence of this side chain, i.e., the W243A mutant receptor, such agonist such as **12** bound but failed to activate the $A_3$AR.[29] Thus, at least within the limited set of adenosine analogues examined (i.e., $N^6$-3-iodobenzyl analogues and 5′-uronamide analogues) this model distinguished the structural bases for binding and activation processes.

## Discussion

We have demonstrated that certain substitutions of adenosine and adenosine analogues contributed differently to binding and function of $A_3$ARs. Specifically, a 2-chloro group in certain cases lowered efficacy. This effect required the presence of an $N^6$-substitution, such as 3-iodobenzyl or cyclopentyl.[9] The $N^6$-unsubstituted 2-Cl analogue **3**, however, was a full agonist.

The $N^6$-(3-iodobenzyl) group itself may lead to reduction of efficacy, even in the absence of multiple substitutions of adenosine. Thus, **4** was a low-efficacy, partial agonist. The combination of 2-chloro and $N^6$-substitution appeared to reduce efficacy further than each modification alone. Thus, **5** was demonstrated to be an antagonist with little if any detectable agonist activity. The $N^6$-cyclopentyl group alone did not reduce efficacy; however, the combination of 2-chloro and $N^6$-cyclopentyl in the present pharmacological system appeared to abolish agonism entirely.[9] Other $N^6$ substitution (e.g., diastereomers **9** and **10**) had no effect on efficacy.

The (*N*)-methanocarba substitution of the ribose ring, resulting in a rigidification of the pseudoribose moiety in an $A_3$AR-preferring conformation,[6] while preserving and/or enhancing binding selectivity, also appeared to reduce $A_3$AR efficacy. Thus, in the 2-H case, compound **17** was less efficacious than **4**. Similarly, in the 2-Cl case, **15** was less efficacious than **3**.

The above-mentioned reduction of efficacy was subject to reversal upon, at least certain, 5′-substitution of the molecule. The 5′-alkylamide group (either *N*-ethyl as in **1**, or *N*-methyl) appeared to restore efficacy. All of the acyclic 5′-amide derivatives, except the 2′,3′-epoxide **13**, were full agonists. Comparison of pairs of compounds differing only in the presence of the 5′-alkylamide group demonstrated that the efficacy-preserving effect of this substituent took precedence over other modifications, i.e., $N^6$-(3-iodobenzyl), 2-halo, and methanocarba, that otherwise reduced efficacy. Thus, among $N^6$-(3-iodobenzyl) analogues **11** was more efficacious than **4**, and for the corresponding 2-chloro analogues **12** was more efficacious than **5**. For $N^6$-(3-iodobenzyl) and (*N*)-methanocarba analogues, **19** was more efficacious than **17**, and for the 2-chloro analogues **20** was more efficacious than **18**. The previously reported[5] full agonism of **20** was consistent with the above patterns, since although this compound is a 2-chloro-(*N*)-methanocarba derivative, it also contained the 5′-*N*-methylamide group.

Partial agonists of ARs are sought for potential therapeutic use, and a number of strategies have been pursued to develop them. A partial agonist of the $A_1$ receptor may be useful to slow AV nodal conduction in the heart and thereby ventricular rate without causing AV block, bradycardia, atrial arrhythmias, or vasodilation.[36] 8-Alkyl substitutions of **4** reduced both affinity and efficacy at the $A_1$AR.[37] IJzerman and co-workers reported that 5′-modification in combination with $N^6$-benzyl substituents known to increase $A_3$AR affinity resulted in the first partial agonists with high affinity at the human $A_3$AR.[8,38] In general, the 2′-and 3′-hydroxy groups of adenosine and its derivatives are important for high affinity binding to and activation of ARs.[2,5,11,26] Modification of the ribose moiety of adenosine resulted in a number of $A_1$-selective compounds with reduced $A_1$AR agonist activity. Removal of the 2′- or 3′-hydroxyl group of full agonists resulted in a drastic reduction of both affinity and efficacy.[25] A similar result, i.e., reduction of efficacy, that was not overcome by the 5′-uronamide modification, was seen at the $A_3$AR with the epoxide derivatives **13** and **21**. The ribose-like moieties of these epoxide derivatives lost the “Northern” conformational character, which would be expected to reduce affinity. Also, formation of this epoxide group precluded the ability for hydrogen bond donation to the receptor as seen in $A_3$AR docking of agonists.

Recently, Hutchinson et al.[39] described that 2-iodo-$N^6$-(*S*-endo-norborn-2-yl)adenosine, a potent, full agonist at the $A_1$AR, had no detectable agonist activity at the $A_{2A}$AR, despite weak, but significant binding affinity. Similarly for the $A_3$AR, the finding that **7** was an antagonist,[9] together with the results of the present study indicated that potent antagonists for both human and rat $A_3$ARs could be identified by modification of the endogenous AR agonist, adenosine.

In previous studies,[11,19] we unsuccessfully sought to convert the agonist **11** into an $A_3$AR antagonist by truncating the ribose moiety. In fact, the present study accomplished that goal with the agonist adenosine, using a more easily attainable, structural modification (2-Cl) and also modifications requiring extensive synthetic schemes, such as the spiro modification of **14**. The antagonism by **14** appears to be related to the rigidity of the spiro-lactam, rather than merely the 4′-alkyl substitution, since a related 4′-methyl analogue[19] was a full $A_3$AR agonist.

Consistent with the present study, it has been demonstrated that **8** is a full agonist for the rat $A_3$AR,[4] while both related xanthine 7-riboside derivatives (the 3′-deoxy and 5′-$CH_2OH$ analogues) were reported to be partial agonists for the rat $A_3$AR. However, a 3′-deoxyadenosine derivative (2-chloro-*N*$^6$-(3-iodobenzyl)-5′-*N*-methylcarbamoyl-3′-deoxyadenosine) was still a full agonist for the $A_3$AR with no affinity change.[11]

Previously, it was found that 2-fluoroadenosine acted as a partial agonist at the $A_{2A}$AR.[40] Our data were consistent with and extended that observation to the $A_3$AR. It is interesting that 2-halo substitution is generally thought to enhance only the affinity of the ligands, while little attention has been paid on their dramatic efficacy-diminishing effects. It remains to be determined if most of the other adenosine derivatives currently used are full agonists for one subtype but are partial, full agonists or antagonists for other AR subtypes. Also, it should be noted that the same compound may behave as a nearly full agonist, a partial agonist, or an antagonist in different tissues. Thus, this classification will also depend on the biological system in which the measurement is made.[41] Actually, a significant number of competitive antagonists of GPCRs currently used as therapeutic agents were first identified as partial agonists or evolved in a structural series from an initially identified partial agonist.[42]

To gain insight into the distinct structural requirements for receptor binding and activation, an $A_3$AR model containing all domains except the C-terminal region were constructed by homology from the X-ray structure of rhodopsin. Ligand docking, taking into account binding of selected derivatives at mutant $A_3$ARs, featured interactions of TM3 (His95) with the adenine moiety and TMs 6 and 7 with the ribose 5′-region. The conserved Trp243 residue in TM6 contributed to the binding of the classical $A_3$AR antagonists[29] but not of adenosine-derived agonists and antagonists; however, this side chain when present displayed a characteristic movement seen exclusively upon docking of agonists. Thus, this residue distinguished components of receptor binding and subsequent activation of the $A_3$AR and furthermore suggested different modes of binding for the two classes of $A_3$AR antagonists. Whether the movement of W243 applies also to other adenosine agonists, such as 5′-$CH_2OH$ derivatives,[9] remains to be examined.

In rhodopsin, both H-bonding networks and van der Waals contacts link the TM helices, stabilizing the ground-state structures.[43] Agonist binding disrupts the intramolecular contact networks, replacing them with a new set that incorporates the ligand itself. The experimental data and crystal structure of rhodopsin suggested that activation by light-induced conformational changes, including the separation of TMs 3 and 6 and increased exposure of the inner faces of TMs 2, 3, 6, and 7, and a decrease in exposure near the

ends of TMs 4 and 5.[44] Specifically, activation of rhodopsin has been predicted to cause a clockwise rotation viewed from the cytoplasmic surface of the endofacial section of TM6, accompanied by a significant outward movement relative to TM3.[45] Although mutation of the conserved residues in various 7TM GPCRs (G protein-coupled receptors) had different effects on receptor function, the conserved W6.48 was typically surrounded by hydrophobic residues from TM3, 6, and 7, as was observed for the thyrotropin releasing hormone (TRH) receptor.[46] This arrangement suggested the formation of an intramolecular TM network to constrain the $A_3$AR, as for the TRH receptor, in an inactive conformation. We speculate that the conserved P6.50 above W6.48 may act as a flexible hinge, and that activation leads to a straightening of TM6, as proposed for rhodopsin.[47]

Thus, our model proposes that movement of W243 and consequently TM6 may be involved in the $A_3$AR activation process,[29] similar to previously postulated movement of GPCRs upon activation.[33,35] Flexibility of the adenosine 5′-position, as well as the 3′-position, which was diminished in (*N*)-methanocarba, spiral, and epoxide analogues, and characteristic ribose binding at TM6 and TM7 appeared to be required for activation of the $A_3$AR. We speculate that the introduction of rigidity in the ribose ring-constrained analogues might be responsible for the reduction of efficacy at the $A_3$AR, thus transforming agonists into antagonists. Other analogues lacking ribose ring constraints, i.e., containing 2-Cl and $N^6$-substitutions, also displayed reduced efficacy, which could not be explained in terms of reduced flexibility. A parallel hypothesis for reduced efficacy is that these particular adenine modifications increased the binding affinity in a way that consequently made it energetically more difficult to twist TM6. While $A_3$AR antagonists were reported to display a high correlation ($r^2 = 0.99$) between functional potency and $A_3$AR binding affinity,[48] the correlation between agonistic potency and binding affinity was weaker. A correlation coefficient ($r^2$) of 0.79 was calculated for the present set of agonists. While there may be many factors responsible for this variation, it is possible that in some cases higher affinity of the complex may limit the ability to activate the receptor through geometric constraint. In addition, there was evidence for an electronic component of the efficacy-reducing effects of adenine substitutions, since the electron-withdrawing 2-F substitution[40] of **2** produced a partial $A_3$AR agonist.

In conclusion, the present study provided new insights into the ligand-$A_3$AR interaction, especially different binding properties of nucleoside agonists and antagonists interacting with Trp243 and at the 5′-position with TM6 and TM7. Furthermore, based on structural considerations we have synthesized and characterized adenosine-derived antagonists and partial agonists for $A_3$ARs, including the rat homologue. Thus, while most $A_3$AR antagonists reported are nonadenosine derivatives of low aqueous solubility, we conclude that it is possible to design potent and more hydrophilic nucleoside-based antagonists of both human and rat $A_3$ARs, such as the highly $A_3$AR selective antagonist **14** or the less selective, but more potent **5**. Selective $A_3$ antagonism independent of species has long been sought, and partial agonism at this receptor may prove to be equally important, especially in light of the therapeutic interest in activation of $A_3$ receptors (cancer, cardioprotection, cerebroprotection).[1,2,9,10,62] Additional structural modification of adenosine may provide further increases in species-independent potency and selectivity. The existence of $A_3$AR

inverse agonists is yet to be demonstrated, and should be sought among diverse antagonist structures, including adenosine derivatives.

## Experimental Procedures

### Chemical Synthesis.

Compound **12** was purchased from Sigma (St. Louis, MO), and **18** was prepared as reported.[5,6] Other chemicals were from Aldrich (Milwaukee, WI) and of analytical grade. $^1$H NMR spectra were recorded using a Varian Gemini-300 spectrometer. High-resolution FAB (fast atom bombardment) mass spectra were taken with a JEOL SX102 spectrometer using nitrobenzoic acid as matrix.

Purity of compounds **13** (90%), **14** (99%), and **21** (93%) was determined using a Hewlett-Packard 1090 HPLC apparatus (detector at 260 nm) equipped with an SMT OD-5–60 RP–C18 analytical column (250 × 4.6 mm; Separation Methods Technologies, Inc., Newark, DE) in two linear gradient solvent systems: System A was 0.1 M triethylammonium acetate/$CH_3CN$ from 95/5 to 40/60 in 20 min and the flow rate was of 1 mL/min; system B was 5 mM tetrabutylammonium phosphate/$CH_3CN$ from 80/20 to 40/60 in 20 min and the flow rate was 1 mL/min.

### {5-[2-Chloro-6-(3-iodo-benzylamino)-purin-9-yl]-3-oxatricyclo[4.1.0.0$^{2,4}$]hept-1-yl}-methanol (21).

A suspension of **18** (100 mg, 0.189 mmol) in acetonitrile (4 mL) was treated with acetonitrile/water (100:1, 0.4 mL) and α-acetoxyisobutyryl bromide (0.11 mL, 0.758 mmol), and the resulting mixture was stirred at room temperature for 1 h. A clear solution resulted after 45 min, and a white precipitate was formed. Aqueous sodium bicarbonate was added and the mixture was extracted with ethyl acetate. Treatment of the crude mixture from the combined organic phase with Amberlite IRA-400 ($OH^-$) resin in dry methanol (4 mL) gave 40.6 mg of 2′,3′-anhydroadenosine derivative **21**, in 42% yield after purification on silica gel column chromatography($CHCl_3$/MeOH = 20:1).

$^1$H NMR ($CD_3OD$-$d_6$) $\delta$ 0.82 (m, 1H), 1.40 (t, 1H, $J$ = 4.8 Hz), 1.83 (m, 1H), 3.72 (d, 1H, $J$ = 2.4 Hz, H-3′), 3.79 (ps d, 1H, $J$ = 11.7 Hz, H-5′), 3.93 (d, 1H, $J$ = 2.4 Hz, H-2′), 4.06 (ps d,1H, $J$ = 11.7 Hz, H-5′), 4.72 (s, 1H, H-1′), 4.78 (s, 2H, NH$\underline{CH_2}$-), 7.10 (t, 1H, $J$ = 7.8 Hz, 5”-H), 7.41 (d, 1H, $J$ = 7.5 Hz, 4” or 6”-H), 7.62 (d, 1H, $J$ = 7.5 Hz, 4” or 6”-H), 7.79, (s, 1H, 2”-H), 8.27 (s, 1H, H-8). MS (FAB) $m/z$ = 510 ($M^+$ + 1). HRMS (FAB) for $C_{18}H_{17}ClIN_6O_3$ (M+H): calcd 510.0194, found 510.0185.

### 4-[2-Chloro-6-(3-iodo-benzylamino)-purin-9-yl]-3,6-dioxa-bicyclo[3.1.0]hexane-2-carboxylic acid methylamide(13).

Compound **12** (4.6 mg, 0.008 mmol) was suspended in acetonitrile (0.2 mL) and treated with 5 μL of α-acetoxyisobutyryl bromide. After the sample was stirred for 1 h at room temperature, the mixture was treated with 5% of sodium bicarbonate (5 mL), and stirring was continued for 1 min. The solution was extracted with ethyl acetate and the organic layer was washed once with water and dried over magnesium sulfate. After evaporation of the

solvent, the crude intermediate **23** was purified on a preparative TLC plate (silica, 2000$\mu$ thickness, eluting with methanol/chloroform in a ratio of 1:4). NMR ($CDCl_3$): d 8.24 (br, s, 1H), 7.75 (s, 1H), 7.64 (d, $J$ = 8.0 Hz, 1H), 7.35 (d, $J$ = 7.7 Hz, 1H), 7.09 (t, $J$ = 7.7 Hz, 1H), 6.34 (b, 1H), 6.20 (d, $J$ = 2.2 Hz, 1H), 5.69 (m, 1H), 4.88 (d, $J$ = 4.1 Hz, 1H), 4.78 (b, 2H), 4.67 (m, 1H), 2.93 (d, $J$ = 4.7 Hz, 3H), 2.19 (s, 3H). FAB-MS: $m/z$ (relative intensity) 649.0 (M+1, 2.2), 651.0 (M+3, 2.6), 391.3 (15), 73.1 (100), 57.1 (30), 43.0 (20).

Intermediate **23** was dissolved in methanol and treated with Amberlite IRA-400 ($OH^-$) resin. The product **13** was purified using preparative TLC as a white amorphous solid. NMR ($CDCl_3$): d 7.78–7.70 (m, 2H), 7.64 (d, $J$ = 8.0 Hz, 1H), 7.35 (d, $J$ = 7.1 Hz, 1H), 7.09 (t, $J$ = 7.7 Hz, 1H), 6.36 (s, 1H), 6.24 (b, 1H), 6.07 (b, 1H), 4.78 (b, 1H), 4.69 (s, 1H), 4.59 (d, $J$ = 2.5 Hz, 1H), 4.07 (d, $J$ = 2.5 Hz, 1H), 2.64 (d, $J$ = 4.9 Hz, 3H). FAB-MS: $m/z$ (relative intensity) 527.1 ($M^+$ + 1, 5), 119.0 (100), 85.0 (60). HRMS (FAB) for $C_{19}H_{18}ClIN_5O_2$ (M+H): calcd 527.0095, found 527.0091.

### Molecular Modeling.

All calculations were performed on a Silicon Graphics Octane workstation (300 MHz MIPS R12000 (IP30) processor). All ligand structures were constructed using the “Sketch Molecule” of SYBYL 6.7.1.[49] A random search for compounds **5**, **12**, and **14** was performed to obtain thermally stable conformations. The options of random search for all rotatable bonds were 3,000 iteration, 3 kcal energy cutoffs, and chirality checking. In all cases, MMFF force field[50] and charge were applied using distance-dependent dielectric constants and conjugate gradient method until the gradient reached to 0.05 kcal/mol/Å. After clustering the low energy conformers from the result of the conformational search, the representative ones from all groups were re-optimized by semiempirical molecular orbital calculations using the PM3 method in the MOPAC 6.0 package.[51]

A human $A_3$AR model was built using homology modeling from the recently published X-ray structure of bovine rhodopsin[31] as we previously described.[32] Multiple-sequence alignment data of selected G protein-coupled receptors were used for the construction of human $A_3$AR TM domains.[52] For the model of the second extracellular loop, EL2, two beta-sheet domains in rhodopsin were first aligned including the disulfide bond between Cys83 and Cys166 and then other parts were added or deleted. To construct the N-terminal region, intra and extracellular loops, each alignment was manually adjusted preserving the overall shape of loop. Acetyl and *N*-methyl amide groups blocked the N-terminal and C-terminal region, respectively. All helices with backbone constraints and loops were minimized separately. After combining together, all structures were reminimized initially with backbone constraints in the secondary structure and then without any constraints. The Amber all-atom force field[53] and the conjugate gradient method with a fixed dielectric constant of 4.0 were used for all calculations, terminating when the gradient reached 0.05 kcal/mol/Å.

For the conformational refinement of the $A_3$AR, the optimized structures were then used as the starting point for subsequent 50 ps Molecular Dynamics (MD), during which the protein backbone atoms in the secondary structures were constrained as in the previous step. The options of MD at 300 K with 0.2 ps coupling constant were a time step of 1 fs and a

nonbonded update every 25 fs. The lengths of bonds with hydrogen atoms were constrained according to the SHAKE algorithm.[54] The average structure from the last 10 ps trajectory of MD was re-minimized with backbone constraints in the secondary structure and then without all constraints.

For the accuracy of 3D $A_3$AR model, the distribution of the main chain torsion angles $\varphi$ and $\psi$ was examined in a Ramachandran plot, and all $\omega$ angles for the peptide planarity were measured. The chirality of all $C_\alpha$ atoms, which in naturally occurring amino acids is of the L-configuration, was checked. RMS deviations between backbone atoms in all helices were compared to the X-ray structure of rhodopsin as a template.

Flexible docking was facilitated through the "FlexiDock" utility in the Biopolymer module of SYBYL 6.7.1. During flexible docking, only the ligand was defined with rotatable bonds. After the hydrogens were added to the receptor, atomic charges were assigned using Kollman All-atom for the protein and calculated using Gasteiger-Hückel for the ligand. Hydrogen bonding sites were marked for all residues in the active site and for ligands that were able to act as hydrogen bond donor or acceptor. Ligands were prepositioned in the cavity as a starting point for FlexiDock. Default FlexiDock parameters were set at 3000-generation for genetic algorithms. To increase the binding interaction, the torsion angles of the side chains that directly interacted within 5 Å of the ligands according to the results of FlexiDock were manually adjusted. Finally, the complex structure was minimized using an Amber force field with fixed dielectric constant (4.0), until the conjugate gradient reached 0.1 kcal/mol/Å.

### Pharmacological Methods.

[$^{125}$I]*N*$^6$-(4-amino-3-iodobenzyl)adenosine-5′-*N*-methyluronamide (I-AB-MECA; 2000 Ci/mmol), [$^3$H]8-ethyl-4-methyl-2-phenyl-(8*R*)-4,5,7,8-tetrahydro-1H-imidazo[2,1-i]-purin-5-one (PSB-11, 53 Ci/mmol) and [$^3$H]cyclic AMP (40 Ci/mmol) were from Amersham Pharmacia Biotech (Buckinghamshire, UK).

### Cell Culture and Membrane Preparation.

CHO (Chinese hamster ovary) cells expressing recombinant the human $A_3$AR were cultured in DMEM supplemented with 10% fetal bovine serum, 100 units/mL penicillin, 100 $\mu$g/mL streptomycin, 2 $\mu$mol/mL glutamine, and 800 $\mu$g/mL Geneticin. The CHO cells expressing rat $A_3$ARs were cultured in DMEM and F12 (1:1). Cells were harvested by trypsinization. After homogenization and suspension, cells were centrifuged at 500 *g* for 10 min, and the pellet was resuspended in 50 mM Tris·HCl buffer (pH 8.0) containing 10 mM $MgCl_2$, 1 mM EDTA and 0.1 mg/mL CHAPS. The suspension was homogenized with an electric homogenizer for 10 s, and was then recentrifuged at 20000*g* for 20 min at 4 °C. The resultant pellets were resuspended in buffer in the presence of 3 Units/mL adenosine deaminase, and the suspension was stored at −80 °C until the binding experiments. Striatal and forebrain tissues from Wistar rats were homogenized in ice-cold 50 mM Tris·HCl buffer, pH 7.4, using an electric homogenizer. The homogenate was centrifuged at 20000*g* for 10 min at 4 °C, and the pellet was washed in fresh buffer. The final pellet was stored at −80 °C

until the binding experiments. The protein concentration was measured using the Bradford assay.[60]

### Site-Directed Mutagenesis.

The method used was described previously.[29] The protocols used were as described in the QuikChange Site-Directed Mutagenesis kit (La Jolla, CA). Mutations were confirmed by DNA sequencing.

### Transient Expression of Wild Type (WT) and Mutant $A_3$ARs in COS-7 Cells.

COS-7 cells ($10^{-6}$) were grown in 100-mm cell culture dishes containing Dulbecco's modified Eagle's medium supplemented with 10% fetal bovine serum, 100 units/mL penicillin, 100 μg/mL streptomycin, and 2 μmol/mL glutamine. After 24 h, cells were washed with phosphate-buffered saline (with calcium) and then transfected with plasmid DNA (10 μg/dish) using the DEAE-dextran method[55] for 1 h. The cells were then treated with 100 μM chloroquine for 3 h in culture medium and cultured for an additional 48 h at 37 °C and 5% $CO_2$.

### Binding Assay using [$^{125}$I]4-amino-3-iodobenzyl)adenosine-5′-*N*-methyluronamide.

For competitive binding assay, each tube contained 50 μL of membrane suspension (20 μg of protein), 25 μL of [$^{125}$I]$N^6$-(4-amino-3-iodobenzyl)adenosine-5′-*N*-methyluronamide (1.0 nM), and 25 μL of increasing concentrations of the test ligands in Tris·HCl buffer (50 mM, pH 8.0) containing 10 mM $MgCl_2$, 1 mM EDTA. Nonspecific binding was determined using 10 μM of **12** in the buffer. The mixtures were incubated at 37 °C for 60 min. Binding reactions were terminated by filtration through Whatman GF/B filters under reduced pressure using a MT-24 cell harvester (Brandell, Gaithersburgh, MD). Filters were washed three times with 9 mL of ice-cold buffer. Radioactivity was determined in a Beckman 5500B γ-counter.

### Cyclic AMP Accumulation Assay.

Intracellular cyclic AMP levels were measured with a competitive protein binding method.[56,57] CHO cell that expressed recombinant human and rat $A_3$ARs were harvested by trypsinization. After centrifugation and resupension in medium, cells were planted in 24-well plates in 1.0 mL of medium. After 24 h, the medium was removed and cells were washed three times with 1 mL of DMEM, containing 50 mM HEPES, pH 7.4. Cells were then treated with agonists and/or test compounds in the presence of rolipram (10 μM) and adenosine deaminase (3 units/mL). After 45 min, forskolin (10 μM) was added to the medium, and incubation was continued an additional 15 min. The reaction was terminated by removing the supernatant, and cells were lysed upon the addition of 200 μL of 0.1 M ice-cold HCl. The cell lysate was resuspended and stored at −20 °C. For determination of cyclic AMP production, protein kinase A (PKA) was incubated with [$^3$H]cyclic AMP (2 nM) in $K_2HPO_4$/EDTA buffer ($K_2HPO_4$, 150 mM; EDTA, 10 mM), 20 μL of the cell lysate, and 30 μL 0.1 M HCl or 50 μL of cyclic AMP solution (0–16 pmol/200 μL for standard curve). Bound radioactivity was separated by rapid filtration through Whatman GF/C filters

and washed once with cold buffer. Bound radioactivity was measured by liquid scintillation spectrometry.

### Effects of a GTP Analogue on the Competition of Tritiated Antagonist Binding to the Human $A_3$AR by Adenosine Derivatives.

The procedure used has been described previously.[23,58] Briefly, [$^3$H]8-ethyl-4-methyl-2-phenyl-(8*R*)-4,5,7,8-tetrahydro-1H-imidazo[2,1-i]-purin-5-one (5 nM) was incubated membranes (80 $\mu$g of protein) from CHO cells expressing the human $A_3$AR in the absence and presence of GTP$\gamma$S (100 $\mu$M) and increasing concentrations of test compounds in a total assay volume of 400 $\mu$L at 25 °C for 60 min. Bound radioactivity was separated by rapid filtration through Whatman GF/C filters and washed once with cold buffer.

### Statistical Analysis.

Binding and functional parameters were estimated using GraphPAD Prism software (GraphPAD, San Diego, CA). $IC_{50}$ values obtained from competition curves were converted to $K_i$ values using the Cheng-Prusoff equation.[59] Data were expressed as mean ± standard error.

## Supplementary Material

Refer to Web version on PubMed Central for supplementary material.

## Acknowledgment.

We thank Dr. Bruce Liang (University of Connecticut) and Dr. John Daly (NIDDK) for helpful discussions, Dr. Gary Stiles (Duke University) for the gifts of CHO cells expressing the human and rat $A_3$ARs, and Prof. Christa Müller (University of Bonn, Germany) for providing [$^3$H]8-ethyl-4-methyl-2-phenyl-(8*R*)-4,5,7,8-tetrahydro-1H-imidazo[2,1-i]-purin-5-one.Z.-G.G. thanks Gilead Sciences (Foster City, CA) for financial support. We thank Dr. Neli Melman for technical assistance.

## References

(1). Jacobson KA; Knutsen LJS P1 and P2 purine and pyrimidine receptors. In Purinergic and Pyrimidinergic Signaling I; Handbook of Experimental Pharmacology, Vol. 151/I; Abbracchio MP, Williams M, Eds.; Springer-Verlag: Berlin, Germany, 2001; pp 129–175.

(2). Müller CE Adenosine receptor ligands-recent developments part I. Agonists. Curr. Med. Chem 2000, 7, 1269–1288. [PubMed: 11032971]

(3). Daly JW; Padgett W; Thompson RD; Kusachi S; Bugni WJ; Olsson RA Structure-activity relationships for $N^6$-substituted adenosines at a brain $A_1$-adenosine receptor with a comparison to an A2-adenosine receptor regulating coronary blood flow. Biochem. Pharmacol 1986, 35, 2467–2481. [PubMed: 3017353]

(4). Kim HO; Ji X.-d.; Siddiqi SM; Olah ME; Stiles GL; Jacobson KA 2-Substitution of $N^6$-benzyladenosine-5′-uronamides enhances selectivity for $A_3$-adenosine receptors. J. Med. Chem 1994, 37, 3614–3621. [PubMed: 7932588]

(5). Lee K; Ravi RG; Ji X.-d.; Marquez VE; Jacobson KA Ring-constrained (N)methanocarba-nucleosides as adenosine receptor agonists: Independent 5′-uronamide and 2′-deoxy modifications. Biorg. Med. Chem. Lett 2001, 11, 1333–1337.

(6). Jacobson KA; Ji X-d.; Li A-H; Melman N; Siddiqui MA; Shin K-J; Marquez VE; Ravi RG Methanocarba Analogues of Purine Nucleosides as Potent and Selective Adenosine Receptor Agonists. J. Med. Chem 2000, 43, 2196–2203. [PubMed: 10841798]

(7). van der Wenden EM; Carnielli M; Roelen HCPF; Lorenzen A; von Frijtag Drabbe Künzel JK; IJzerman AP 5′-substituted adenosine analogues as new high-affinity partial agonists for the adenosine $A_1$ receptor. J. Med. Chem 1998, 41, 102–108. [PubMed: 9438026]

(8). van Tilburg EW; von Frijtag Drabbe Künzel J; de Groote M; Vollinga RC; Lorenzen A; IJzerman AP $N^6$,5′-Disubstituted adenosine derivatives as partial agonists for the human adenosine $A_3$ receptor. J. Med. Chem 1999, 42, 1393–1400. [PubMed: 10212125]

(9). Gao ZG; Jacobson KA, 2-Chloro-$N^6$-cyclopentyladenosine, adenosine $A_1$ receptor agonist, antagonizes the adenosine $A_3$ receptor, Eur. J. Pharmacol 2002, 443, 39–42. [PubMed: 12044789]

(10). Baraldi PG; Cacciari B; Romagnoli R; Merighi S; Varani K; Borea PA; Spalluto G $A_3$ Adenosine receptor ligands; history and perspectives. Med. Res. Rev 2000, 20, 103–128. [PubMed: 10723024]

(11). Jacobson KA; Siddiqi SM; Olah ME; Ji X-d.; Melman N; Bellamkonda K; Meshulam Y; Stiles GL; Kim HO Structure-activity relationships of 9-alkyladenine and ribose-modified adenosine derivatives at rat $A_3$ adenosine receptors. J. Med. Chem 1995, 38, 1720–1735. [PubMed: 7752196]

(12). Park KS; Hoffmann C; Kim HO; Padgett WL; Daly JW; Brambilla R; Motta C; Abbracchio MP; and Jacobson KA Activation and desensitization of rat $A_3$-adenosine receptors by selective adenosine derivatives and xanthine-7-ribosides. Drug Dev. Res 1998, 44, 97–105. [PubMed: 23487508]

(13). Nandanan E; Jang SY; Moro S; Kim H; Siddiqi MA; Russ P; Marquez VE; Busson R; Herdewijn P; Harden TK; Boyer JL; Jacobson KA Synthesis, biological activity, and molecular modeling of ribose-modified adenosine bisphosphate analogues as $P2Y_1$ receptor ligands. J. Med. Chem 2000, 43, 829–842. [PubMed: 10715151]

(14). Zimmerman DM; Leander JD Selective opioid receptor agonists and antagonists: research tools and potential therapeutic agents. J. Med. Chem 1990, 33, 895–902. [PubMed: 2155322]

(15). Holst B; Zoffmann S; Elling CE; Hjorth SA; Schwartz TW Steric hindrance mutagenesis versus alanine scan in mapping of ligand binding sites in the tachykinin NK1 receptor. Mol. Pharmacol 1998, 53, 166–175. [PubMed: 9443945]

(16). Robins MJ; Hansske F; Low NH; Park JI A mild conversion of vicinal diols to alkenes. Efficient transformation of ribonucleosides into 2′-ene and 2′,3′-dideoxynucleosides. Tetrahedron Lett. 1984, 25, 367–370.

(17). Hansske F; Robins MJ Regiospecific and stereoselective conversion of ribonucleosides to 3′-deoxynucleosides. A high yield three-stage synthesis of cordycepin from adenosine. Tetrahedron Lett. 1985, 26, 4295.

(18). Russell AF; Greenberg S; Moffatt JG Reaction of 2-acyl-oxyisobutyryl halides with nucleosides. II. Reaction of adenosine. J. Am. Chem. Soc 1973, 95, 4025. [PubMed: 4710061]

(19). Siddiqi SM; Jacobson KA; Esker JL; Melman N; Tiwari KN; Secrist JA; Schneller SW; Cristalli G; Johnson CA; IJzerman APSearch for new purine- and ribose-modified adenosine analogues as selective agonists and antagonists at adenosine receptors. J. Med. Chem 1995, 38, 1174–1188. [PubMed: 7707320]

(20). Johnson CR; Esker JL; Van Zandt MC Chemoenzymic synthesis of 4-substituted riboses. *S*-(4′-Methyladenosyl)-L-homocysteine. J. Org. Chem 1994, 59, 5854–5855.

(21). Vorbrüggen H; Ruh-Pohlenz C Synthesis of nucleosides. Org. React 2000, 55, 1–630.

(22). Jacobson KA; Park KS; Jiang JL; Kim Y-C; Olah ME; Stiles GL; Ji X-d. Pharmacological characterization of novel $A_3$ adenosine receptor-selective antagonists. Neuropharmacology 1997, 36, 1157–1165 [PubMed: 9364471]

(23). Gao ZG; Van Muijlwijk-Koezen JE; Chen A; Müller CE; IJzerman AP; Jacobson KA Allosteric modulation of $A_3$ adenosine receptors by a series of 3-(2-pyridinyl)isoquinoline derivatives. Mol. Pharmacol 2001, 60, 1057–1063. [PubMed: 11641434]

(24). Arunlakshana O; Schild HO Some quantitative uses of drug antagonists. Br. J. Pharmacol. Chemother 1959, 14, 48–58. [PubMed: 13651579]

(25). van der Wenden EM; von Frijtag Drabbe Künzel JK; Mathot RA; Danhof M; IJzerman AP; Soudijn W Ribose-modified adenosine analogues as potential partial agonists for the adenosine receptor. J. Med. Chem 1995, 38, 4000–4006. [PubMed: 7562934]

(26). Lohse MJ; Klotz KN; Diekmann E; Friedrich K; Schwabe U2′, 3′-Dideoxy-$N^6$-cyclohexyladenosine: an adenosine derivative with antagonist properties at adenosine receptors. Eur. J. Pharmacol 1988, 156, 157–160. [PubMed: 3208837]

(27). Lorenzen A; Guerra L; Vogt H; Schwabe U Interaction of full and partial agonists of the $A_1$ adenosine receptor with receptor/G protein complexes in rat brain membranes. Mol. Pharmacol 1996, 49, 915–926. [PubMed: 8622642]

(28). Müller CE; Diekmann M; Thorand M; Ozola V [$^3$H]8-Ethyl-4-methyl-2-phenyl-(8R)-4,5,7,8-tetrahydro-1H-imidazo[2,1-i]-purin-5-one ([$^3$H]PSB-11), a Novel High-Affinity Antagonist Radioligand for Human $A_3$ Adenosine Receptors. Bioorg. Med. Chem. Lett 2002, 12, 501–503. [PubMed: 11814828]

(29). Gao ZG; Chen A; Barak D; Kim SK; Müller CE; Jacobson KA Identification by site-directed mutagenesis of residues involved in ligand recognition and activation of the human $A_3$ adenosine receptor. J. Biol. Chem 2002, 277, 19056–19063. [PubMed: 11891221]

(30). Varani K; Merighi S; Gessi S; Klotz KN; Leung E; Baraldi G; Cacciari B; Romagnoli R; Spalluto G; Borea PA [$^3$H]MRE 3008F20: a novel antagonist radioligand for the pharmacological and biochemical characterization of human A3 adenosine receptors. Mol. Pharmacol 2000, 57, 968–975. [PubMed: 10779381]

(31). Palczewski K; Kumasaka T; Hori T; Behnke CA; Motoshima H; Fox BA; Le Trong I; Teller DC; Okada T; Stenkamp TE; Yamamoto M; Miyano M Crystal Structure of Rhodopsin: A G Protein-Coupled Receptor. Science 2000, 289, 739–745. [PubMed: 10926528]

(32). Jacobson KA; Gao ZG; Chen A; Barak D; Kim SA; Lee K; Link A; van Rompaey P; van Calenbergh S; Liang BT Neoceptor Concept Based on Molecular Complementarity in GPCRs: A Mutant Adenosine $A_3$ Receptor with Selectively Enhanced Affinity for Amine-Modified Nucleosides. J. Med. Chem 2001, 44, 4125–4136. [PubMed: 11708915]

(33). Kim J; Wess J; van Rhee AM; Schöneberg T; Jacobson K Site-directed Mutagenesis Identifies Residues Involved in Ligand Recognition in the Human $A_{2a}$ Adenosine Receptor. J. Biol. Chem 1995, 270, 13987–13997. [PubMed: 7775460]

(34). Kim J; Jiang Q; Glashofer M; Yehle S; Wess J; Jacobson KA Glutamate Residues in the Second Extracellular Loop of the Human $A_{2a}$ Adenosine Receptor Are Required for Ligand Recognition. Mol. Pharmacol 1996, 49, 683–691. [PubMed: 8609897]

(35). Jiang Q; van Rhee M; Kim J; Yehle S; Wess J; Jacobson KA Hydrophilic Side Chains in the Third and Seventh Transmembrane Helical Domains of Human $A_{2A}$ Adenosine Receptors Are Required for Ligand Recognition. Mol. Pharmacol 1996, 50, 512–521. [PubMed: 8794889]

(36). Wu L; Belardinelli L; Zablocki JA; Palle V; Shryock JC A partial agonist of the $A_1$-adenosine receptor selectively slows AV conduction in guinea pig hearts. Am. J. Physiol. Heart Circ. Physiol 2001, 280, H334–H343. [PubMed: 11123249]

(37). Roelen H; Veldman N; Spek AL; von Frijtag Drabbe Künzel J; Mathot RA; IJzerman AP $N^6$,C8-disubstituted adenosine derivatives as partial agonists for adenosine $A_1$ receptors. J. Med. Chem 1996, 39, 1463–1471. [PubMed: 8691477]

(38). van Tilburg EW; von Frijtag Drabbe Künzel J; de Groote M; IJzerman AP 2,5′-Disubstituted adenosine derivatives: evaluation of selectivity and efficacy for the adenosine $A_1$, $A_{2A}$, and $A_3$ receptor. J. Med. Chem 2002, 45, 420–429. [PubMed: 11784146]

(39). Hutchinson SA; Baker SP; Scammells PJ New 2,$N^6$-Disubstituted adenosines: potent and selective $A_1$ adenosine receptor agonists. Bioorg. Med. Chem 2002, 10, 1115–1122. [PubMed: 11836122]

(40). Daly JW; Padgett WL Agonist activity of 2- and 5′-substituted adenosine analogues and their $N^6$-cycloalkyl derivatives at $A_1$- and $A_2$-adenosine receptors coupled to adenylate cyclase. Biochem. Pharmacol 1992, 43, 1089–1093. [PubMed: 1554381]

(41). Kenakin TP The Pharmacologic Analysis of Drug-Receptor Interactions; Lippincott-Raven, Philadelphia, New York, 1997.

(42). Harden TK; Boyer JL; Dougherty RW Drug analysis based on signaling responses to G-protein-coupled receptors. J. Recept. Signal Transduct. Res 2001, 2, 167–190.

(43). Teller DC; Okada T; Behnke CA; Palczewski K; Stenkamp RE Advances in determination of a high-resolution three-dimensional structure of rhodopsin, a model of G-protein-coupled receptors (GPCRs). Biochemistry 2001, 40, 7761–7772. [PubMed: 11425302]

(44). Meng EC; Bourne HR Receptor activation: what does the rhodopsin structure tell us? Trends Pharmacol. Sci 2001, 22, 587–593. [PubMed: 11698103]

(45). Lu Z-L; Saldanha JW; Hulme EC Seven-transmembrane receptors: crystals clarify. Trends Pharmacol. Sci 2002, 23, 140–146. [PubMed: 11879682]

(46). Colson A-O; Perlman JH; Jinsi-Parimoo A; Nussenzveig DR; Osman R; Gershengorn MC A hydrophobic cluster between transmembrane helices 5 and 6 constrains the thyrotropin-releasing hormone receptor in an inactive conformation. Mol. Pharmacol 1998, 54, 968–978. [PubMed: 9855624]

(47). Ballesteros JA; Shi L; Javitch JA Structural mimicry in G protein-coupled receptors: Implications of the high-resolution structure of rhodopsin for structure-function analysis of rhodopsin-like receptors. Mol. Pharmacol 2001, 60, 1–19. [PubMed: 11408595]

(48). Baraldi PG; Cacciari B; Moro S; Spalluto G; Pastorin G; Da Ros T; Klotz K-N; Varani K; Gessi S; Borea PA Synthesis, biological activity, and molecular modeling investigation of new pyrazolo[4,3-e]-1,2,4-triazolo[1,5-c]pyrimidine derivatives as human $A_3$ adenosine receptor antagonists. J. Med. Chem 2002, 45, 770–780. [PubMed: 11831890]

(49). Sybyl Molecular Modeling System, version 6.7.1; Tripos Inc., 1969 South Hanley Rd., St. Louis, MO 63144, USA.

(50). Halgren TA; MMFF VII. Characterization of MMFF94, MMFF94s, and other widely available force fields for conformational energies and for intermolecular-interaction energies and geometries. J. Comput. Chem 1999, 20, 730–748. [PubMed: 34376036]

(51). Stewart JJP MOPAC: A semiempirical molecular orbital program. J. Comput.-Aided Mol. Des 1990, 4, 1–105. [PubMed: 2197373]

(52). van Rhee AM; Jacobson KA Molecular architecture of G protein-coupled receptors. Drug Dev. Res 1996, 37, 1–38. [PubMed: 21921973]

(53). Cornell WD; Cieplak P; Bayly CI; Gould IR; Merz KM Jr.; Ferguson DM; Spellmeyer DC; Fox T; Caldwell JW; Kollman PA A second generation force field for the simulation of proteins, nucleic acids and organic molecules. J. Am. Chem. Soc 1995, 117, 5179–5197.

(54). Ryckaert JP; Ciccotti G; Berendsen HJC Numerical integration of the Cartesian equations of motion for a system with constraints: Molecular dynamics of *n*-alkanes.J. Comput. Phys 1977, 23, 327–333.

(55). Cullen BR Use of eukaryotic expression technology in the functional analysis of cloned genes. Methods Enzymol. 1987, 52, 684–704.

(56). Nordstedt C; Fredholm BB A modification of a protein-binding method for rapid quantification of cAMP in cell-culture supernatants and body fluid. Anal. Biochem 1990, 189, 231–234. [PubMed: 2177960]

(57). Post SR; Ostrom RS; Insel PA Biochemical methods for detection and measurement of cyclic AMP and adenylyl cyclase activity. Methods Mol. Biol 2000, 126, 363–374. [PubMed: 10685423]

(58). Gao ZG; Jiang Q; Jacobson KA; IJzerman AP Site-directed mutagenesis studies of human $A_{2A}$ adenosine receptors: involvement of $Glu^{13}$ and $His^{278}$ in ligand binding and sodium modulation. Biochem. Pharmacol 2000, 60, 661–668. [PubMed: 10927024]

(59). Cheng Y-C; Prusoff WH Relationship between the inhibition constant ($K_i$) and the concentration of inhibitor which causes 50% inhibition ($I_{50}$) of an enzymatic reaction. Biochem. Pharmacol 1973, 22, 3099–3108. [PubMed: 4202581]

(60). Bradford MM A rapid and sensitive method for the quantitation of microgram quantities of protein utilizing the principle of protein-dye binding. Anal. Biochem 1976, 72, 248–254. [PubMed: 942051]

(61). Jiang JL; Li A-H; Jang SY; Chang L; Melman N; Moro S; Ji X.-d.; Lobkovsky EB; Clardy JC; Jacobson KA Chiral resolution and stereospecificity of 4-phenylethynyl-6-phenyl-1,4-

dihydropyridine derivatives as selective $A_3$ adenosine receptor antagonists. J. Med. Chem 1999, 42, 3055–3065. [PubMed: 10447949]

(62). Fishman P; Madi L; Bar-Yehuda S; Barer F; Del Valle L; Khalili K Evidence for involvement of Wnt signaling pathway in IB-MECA mediated suppression of melanoma cells. Oncogene 2002, 21, 4060–4064. [PubMed: 12037688]

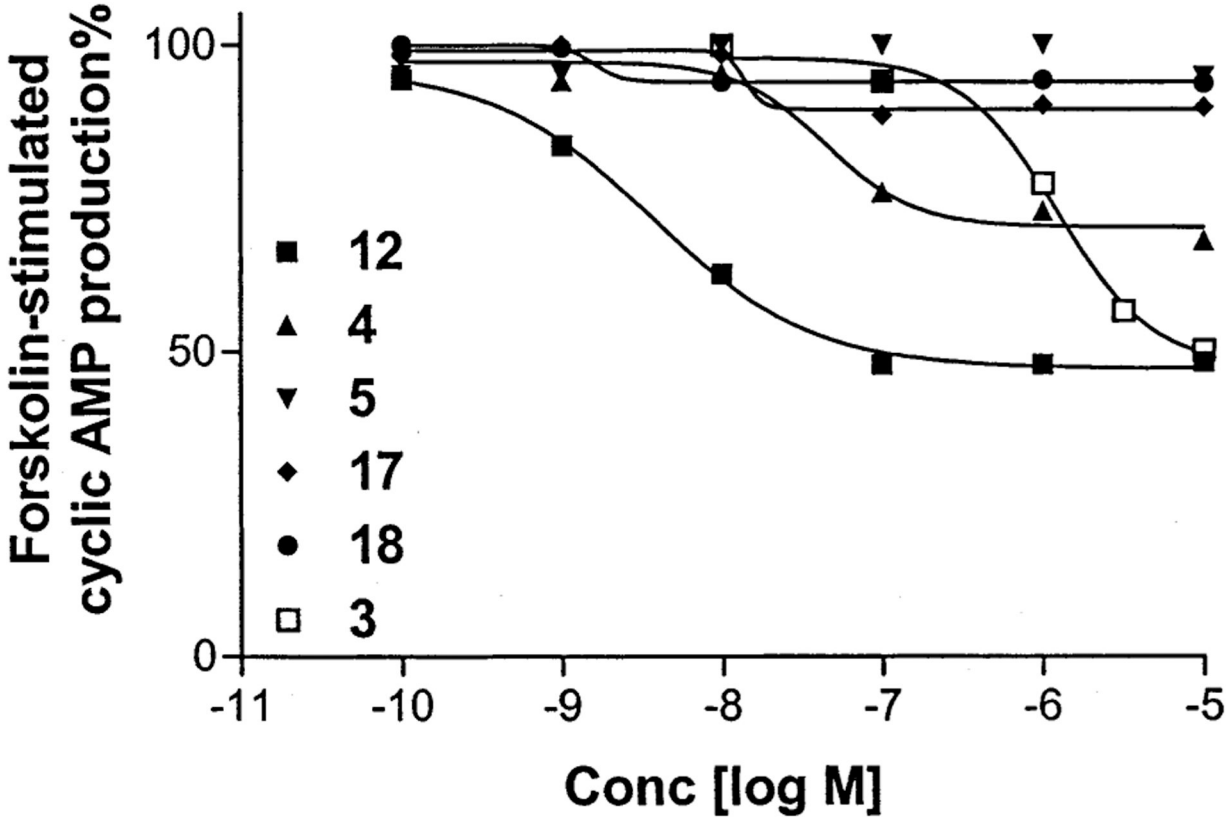


**Figure 1.**

The effects of a series of adenosine derivatives on forskolin-stimulated cyclic AMP accumulation in intact CHO cells expressing the human $A_3$AR. Results shown are from one representative experiment, and the $EC_{50}$ values listed in Table 1 are from 3 to 5 experiments performed in duplicate.

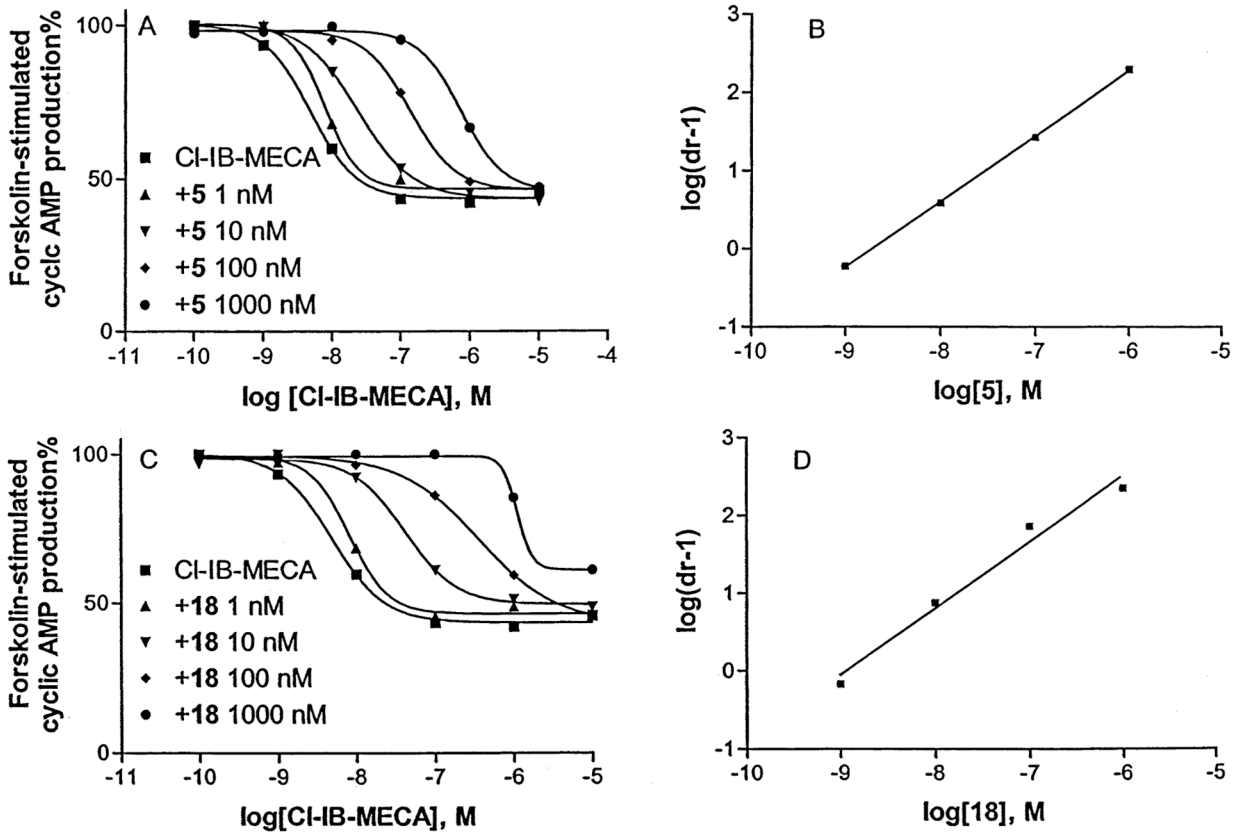


**Figure 2.**

Shift of the dose-response curves inhibition by the agonist **12** of forskolin-stimulated cyclic AMP accumulation in intact CHO cells expressing the human $A_3$AR, in the presence of antagonists **7** (A) and **18** (C). Schild analysis of the data for **7** (B) and **18** (D).

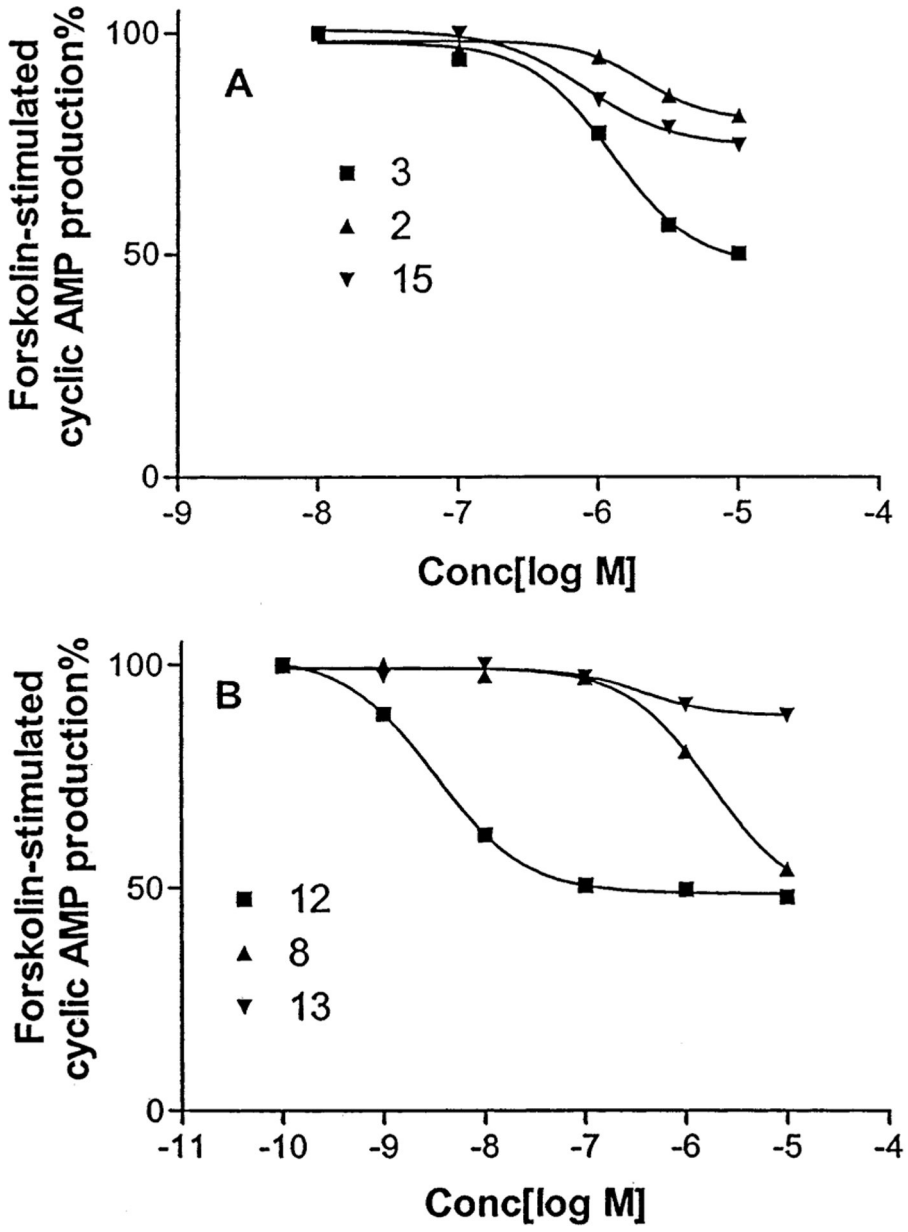


**Figure 3.**

Differential effects of nucleoside 5′-$CH_2OH$ derivatives **2**, **3**, and **15** (A) and 5′-uronamide derivatives **8**, **12**, and **13** (B) on forskolin-stimulated cyclic AMP accumulation in CHO cells expressing the human $A_3AR$. Results shown are from a representative experiment, and the $EC_{50}$ values are listed in Table 1 are calculated from at least three experiments.

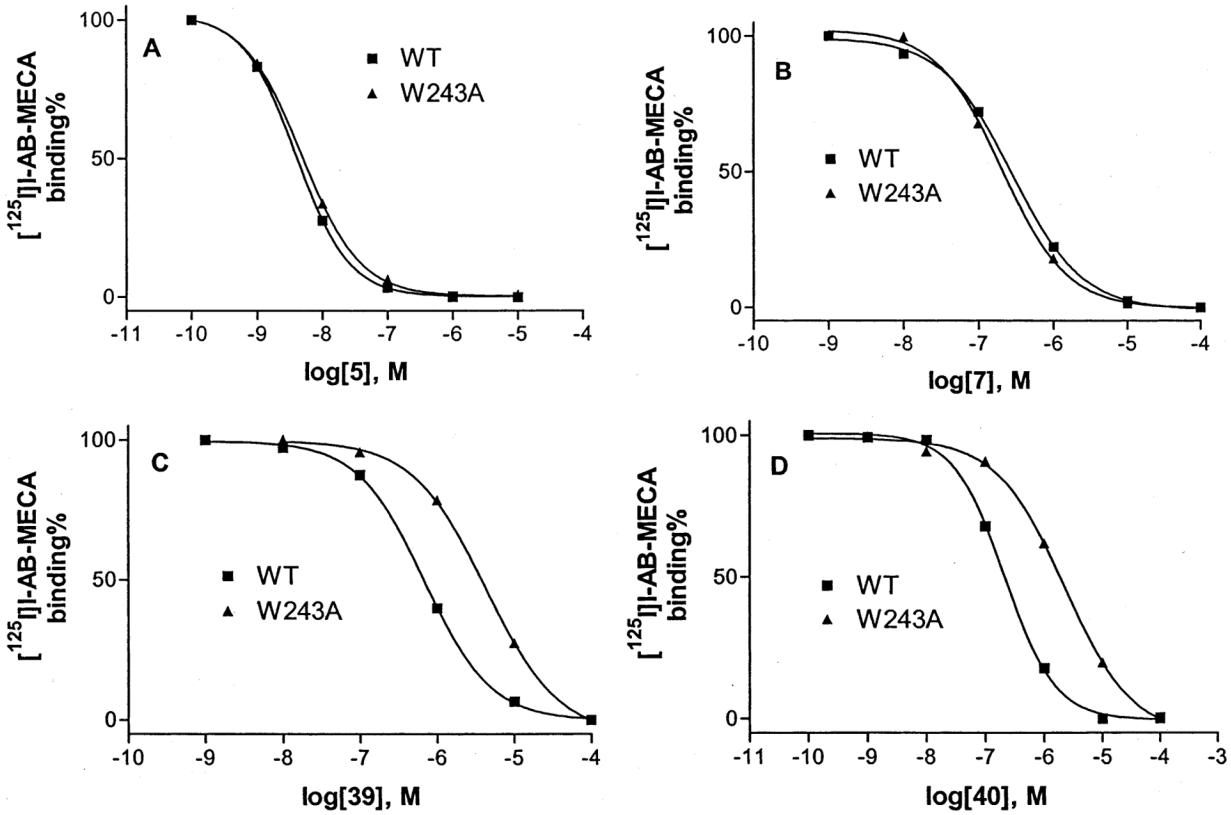


**Figure 4.**

Differential modulation of binding at wild type and W243A mutant human $A_3$ARs for adenosine-derived antagonists (A, **5**; B, **7**) and nonnucleoside antagonists (C, pyridine derivative **39**; D, dihydropyridine derivative **40**). Results shown are from a representative experiment, and the $K_i$ values listed in Table 1 are calculated from three experiments. [$^{125}$I]4-amino-3-iodobenzyl)-adenosine-5′-*N*-methyluronamide, 1 nM. Protein concentration (10–20 $\mu$g of protein).

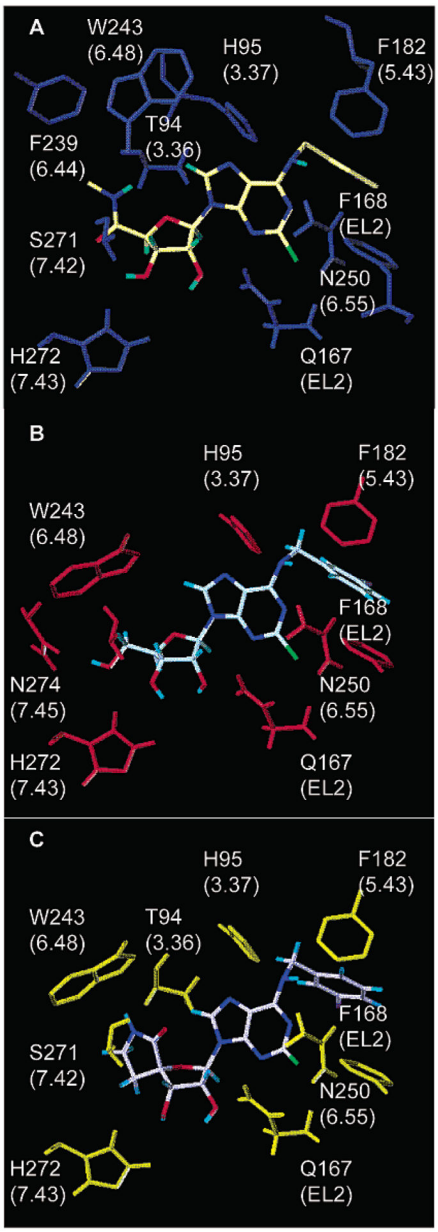


**Figure 5.**

The optimized conformations of the human $A_3$AR following docking of agonist (A) **12** or antagonists (B) **5** and (C) **14**. The ligand molecules were colored according to atom type.

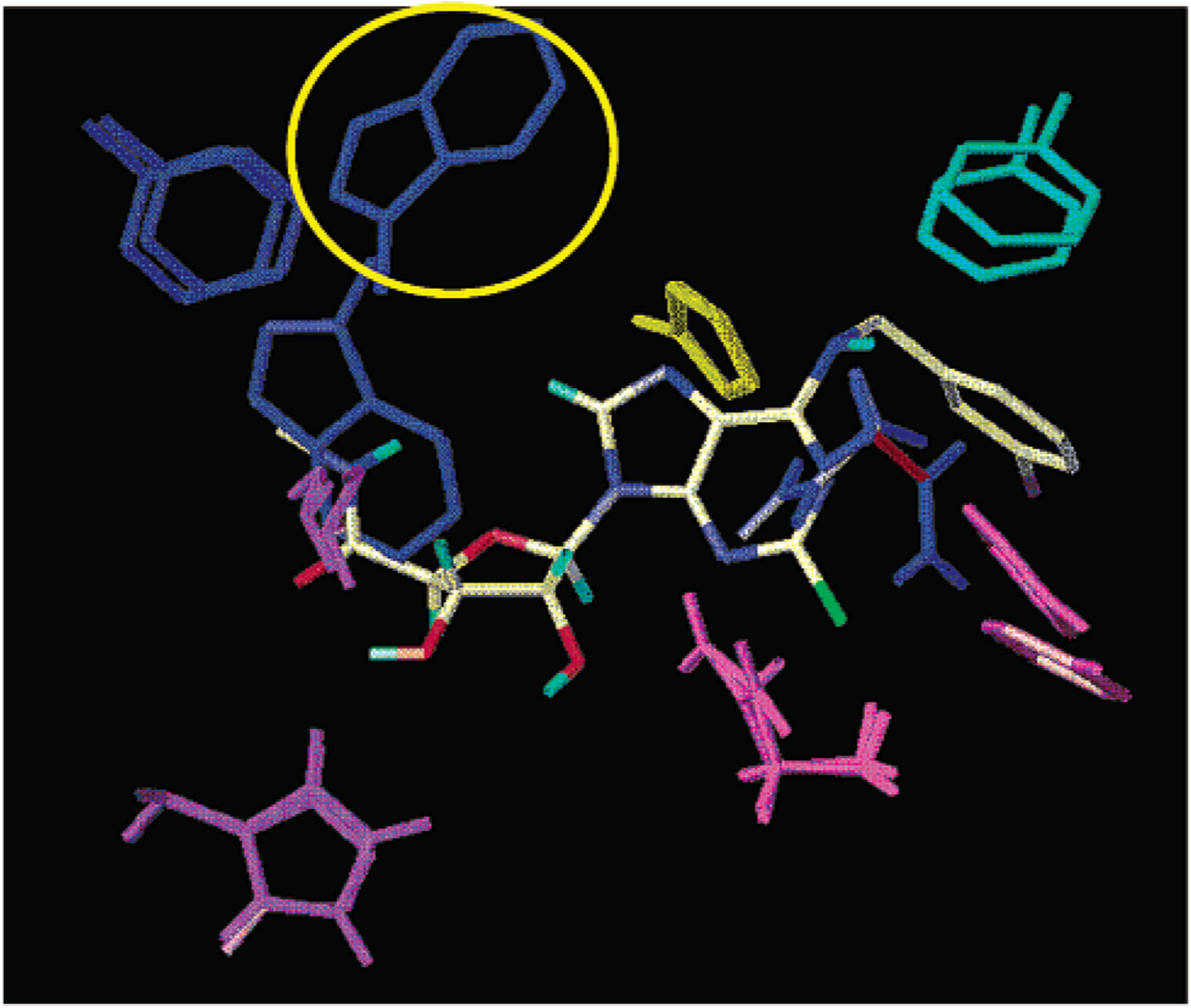

**Figure 6.**

The superimposition of the unoccupied human $A_3$AR model and the complex after binding of full agonist **12**. The orientation of the side chain of W243 (6.48) within the $A_3$AR binding pocket shifted dramatically upon agonist binding (final position circled). The indole rotation is counterclockwise as viewed from the exofacial side. The colors of amino acid side chains were: yellow in TM3 (H95), cyan in TM5 (F182), blue in TM6 (F239, W243), purple in TM7 (H272), and magenta in EL2 (Q167, F168). Upon binding of **12** the orientation ($C_{CO}$-$C_\alpha$-$C_\beta$-$C_\gamma$ dihedral angle) of the W243 side chain shifts from 156.5° to −59.3°. The corresponding angles in Figure 5B,C are 146.5° and 148.1°, respectively.

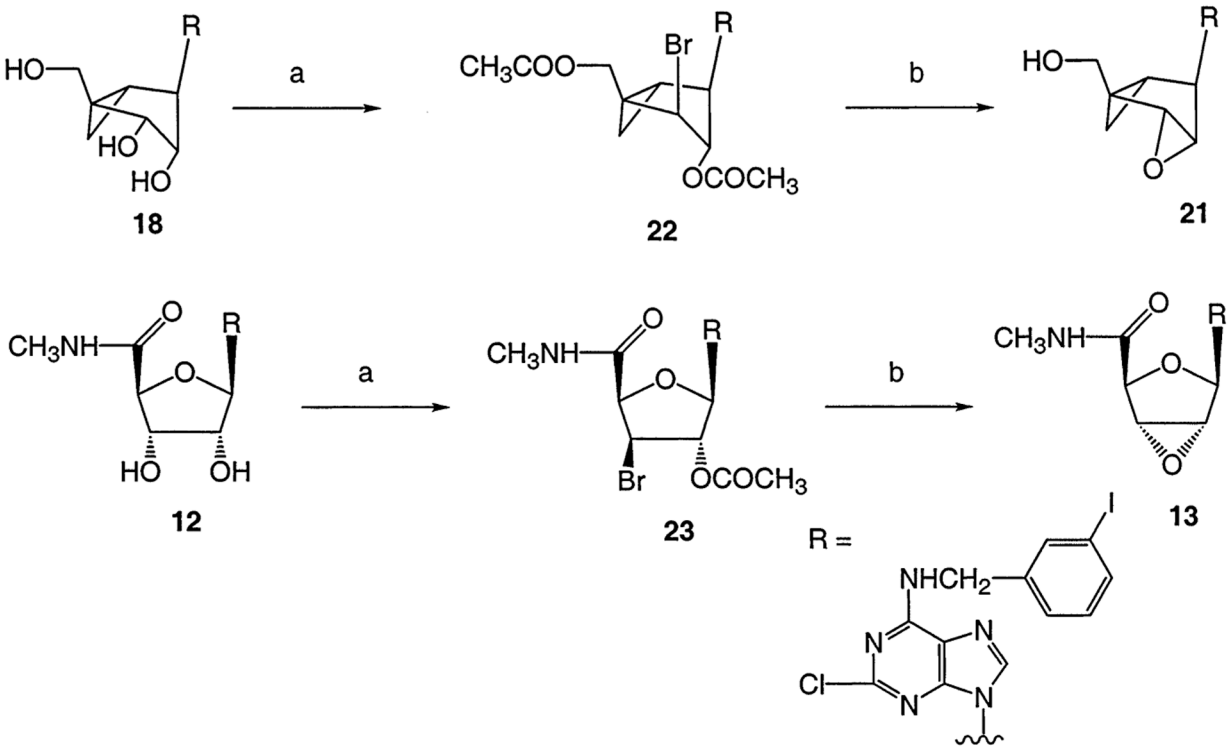


**Scheme 1.**

Synthesis of Ring-Constrained Adenosine Derivatives **21** and **13** Containing 2′,3′-Epoxide Groups[a]

[a]Reagents and conditions: (a) Acetoxyisobutyryl bromide, $CH_3CN$. (b) Amberlite IRA-400 ($OH^-$) resin, MeOH.

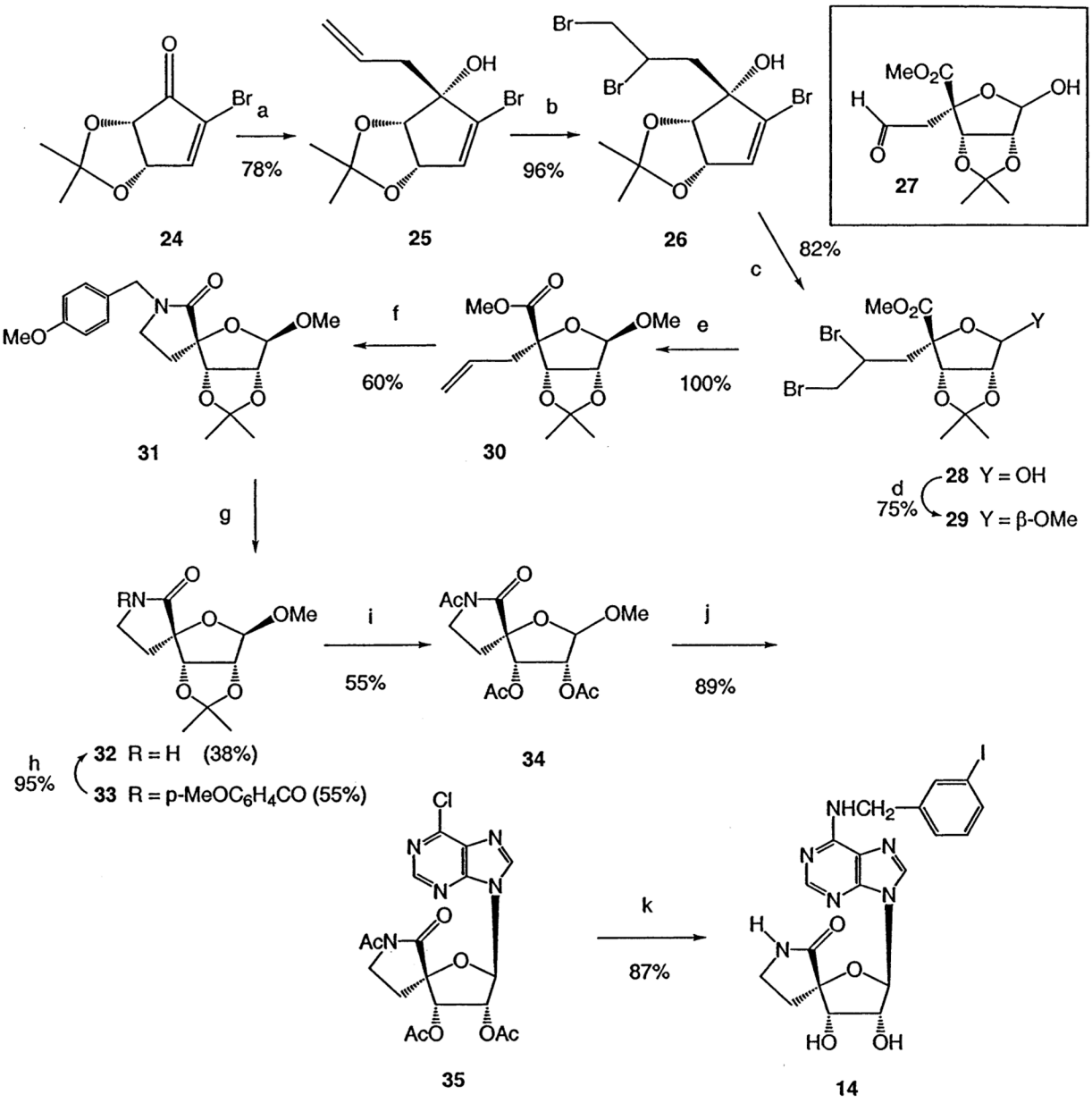


**Scheme 2.**

Synthesis of a Ring-Constrained Spiro Adenosine Derivative **14** Containing a 4′,5′-Lactam Group[a]

[a] Reagents and conditions: (a) allylmagnesium chloride, THF, −78 °C. (b) $Br_2$, $Et_3N$. (c) $O_3$, MeOH/pyridine, −78 °C, then dimethyl sulfide. (d) MeOH, TsOH, 65 °C. (e) Zn, MeOH, 65 °C. (f) (1) $O_3$, $CH_2C1_2$, then dimethyl sulfide; (2) *p*-$MeOC_6H_4CH_2NH_2$, $NaCNBH_3$. (g) ceric ammonium nitrate, $MeCN/H_2O$. (h) $K_2CO_3$, MeOH, 18-crown-6. (i) (1) HC1 (3%), MeOH, 65 °C; (2) $Ac_2O$, $Et_3N$. (j) hexamethyldisilazane, 6-chloropurine, TMSOTf, MeCN, 85 °C. (k) (1) $NH_3$, MeOH, 20 min; (2) 3-iodobenzylamine hydrochloride, $Et_3N$, *t*-BuOH, 85 °C, 6 days.

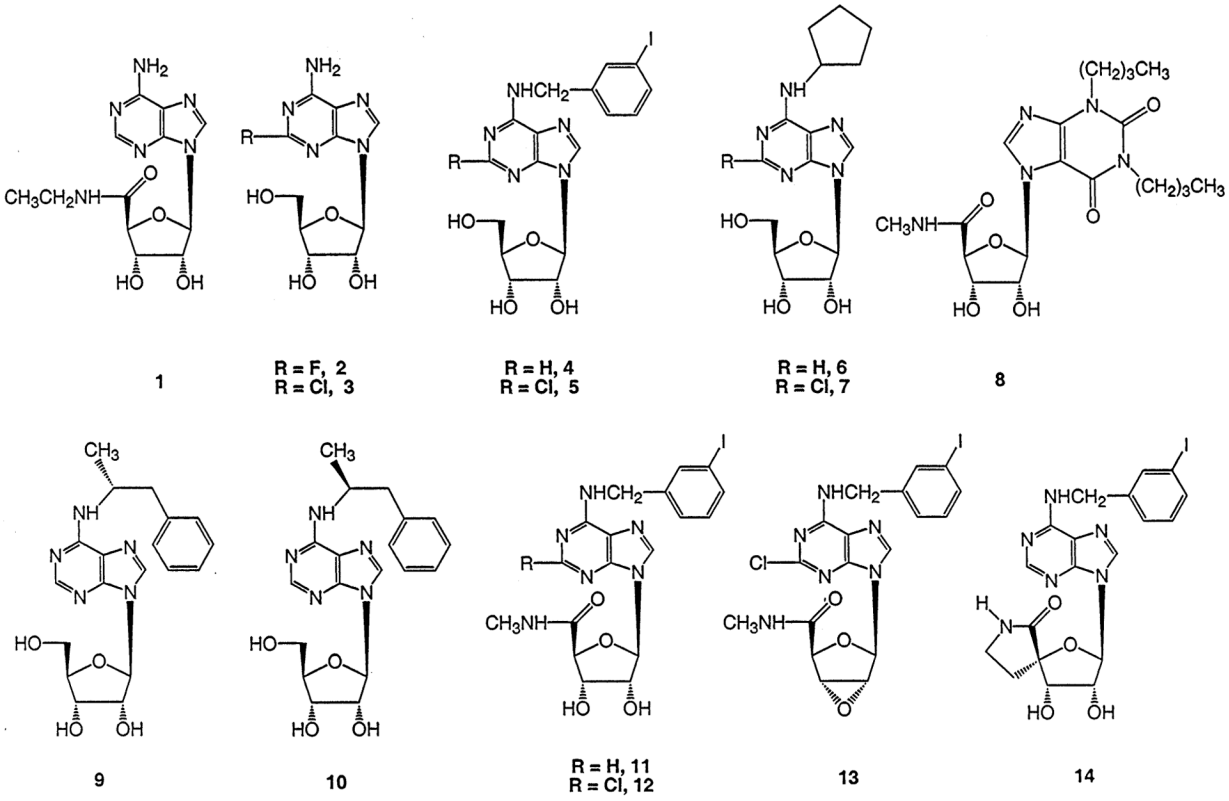


**Chart 1.**

Chemical Structures of Adenosine Derivatives Used in the Present Study and Containing a 9-Ribose Moiety

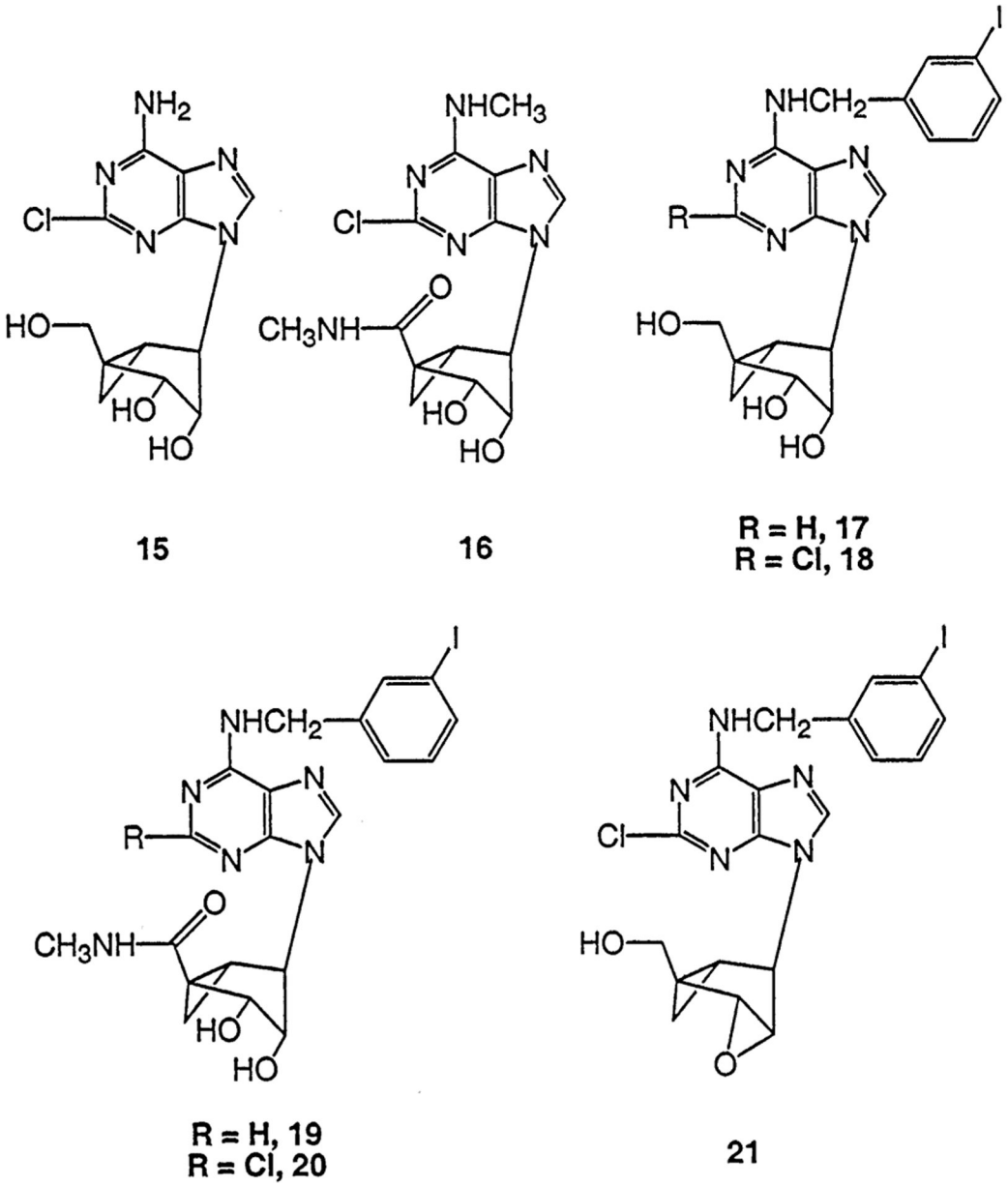


**Chart 2.**

Chemical Structures of Adenosine Derivatives Used in the Present Study and Containing an (*N*)-Methanocarba Moiety

**Table 1.**

Binding and Function of a Series of Adenosine Derivatives at Human $A_3$ Receptors Expressed in CHO Cells[a]

| | $EC_{50}$ (nM) | efficacy (%) | affinity ($K_i$, nM) |
|---|---|---|---|
| **1** | 26 ± 14 | 103 ± 6 | 35 ± 12 |
| **2** | 2660 ± 880 | 31 ± 3 | 99 ± 13 |
| **3** | 1630 ± 610 | 100 ± 7 | 87 ± 24 |
| **4** | 85 ± 13 | 46 ± 8 | 5.8 ± 0.4 |
| **5** | NA | 0 | 1.8 ± 0.1 |
| **6** | 242 ± 47[b] | 97 ± 4 | 72 ± 12[b] |
| **7** | NA | 0 | 38 ± 6[b] |
| **8** | 828 ± 236 | 96 ± 4 | 816 ± 206 |
| **9** | 27 ± 11 | 102 ± 6 | 8.7 ± 0.9 |
| **10** | 210 ± 56 | 97 ± 3 | 68 ± 12 |
| **11** | 3.6 ± 1.3 | 100 | 1.8 ± 0.7 |
| **12** | 2.8 ± 1.4 | 99 ± 6 | 1.4 ± 0.3 |
| **13** | NA | 7 ± 1 | 1100 ± 110 |
| **14** | NA | 0 | 29.3 ± 1.6 |
| **15** | 803 ± 329 | 41 ± 5 | 353 ± 54 |
| **16** | 1.4 ± 0.2 | 104 ± 7 | 3.4 ± 0.6 |
| **17** | NA | 13 ± 1 | 9.2 ± 0.7 |
| **18** | NA | 3 ± 2 | 1.9 ± 0.7 |
| **19** | 5.4 ± 0.9 | 101 ± 5 | 1.3 ± 0.1 |
| **20** | 3.3 ± 1.1 | 103 ± 9 | 2.1 ± 0.4 |
| **21** | NA | 0 | 572 ± 113 |
| **36** | 1.6 ± 0.3 | 103 ± 6 | 1.5 ± 0.2 |
| **37** | 158 ± 28 | 98 ± 5 | 114 ± 16 |

[a]The activation of the human A3 receptor by adenosine derivatives was investigated by examining their effects on forskolin-stiumulated cyclic AMP accumulation in intact CHO cells expressing the human A3AR. Abbreviations: **1** NECA, **5** MRS542, **8** DBXRM, **11** IB-MECA, **12** Cl-IB-MECA, **14** MRS1292, **17** MRS1743, **18** MRS1760, **20** MRS1898, **36** $N^6$-(4-amino-3-iodobenzyl)adenosine-5′-*N*-methyluronamide, **37** 2-[*p*-(carboxyethyl)-phenylethylamino]-5′-*N*-ethylcarboxamidoadenosine. The binding affinity was determined using [$^{125}$I]**36**. Data were from 3 to 5 experiments. NA, not applicable.

[b]Data from Gao and Jacobson.[9]

**Table 2.**

Effects of a Nucleotide GTP$\gamma$S on Ligand Competition Curves for a Tritiated Antagonist Binding to Membranes from CHO Cells Expressing the Human $A_3$AR[a]

| | $K_i$ (nM) | | |
|---|---|---|---|
| | **control** | **+GTP$\gamma$S** | **shift (fold)** |
| **5** | 3.2 ± 0.3 | 3.9 ± 0.4 | 1.2 |
| **7** | 38 ± 6 | 34 ± 7 | 0.9[b] |
| **12** | 1.5 ± 0.2 | 6.3 ± 0.4 | 4.2 |
| **14** | 26 ± 7 | 24 ± 3 | 0.92 |
| **18** | 2.7 ± 0.3 | 4.0 ± 0.3 | 1.5 |
| **38** [b] | 1.2 ± 0.1 | 1.2 ± 0.2 | 1.0 |

[a]Binding was carried out in membranes (80 $\mu$g of protein) of CHO cells stably expressing recombinant the human A3AR. The concentration of [$^3$H]8-ethyl-4-methyl-2-phenyl-(8R)-4,5,7,8-tetrahydro-1H-imidazo[2,1-i]-purin-5-one was 5 nM. The concentration of GTP$\gamma$S used was 100 $\mu$M. Data were expressed as mean ± SEM from three independent experiments.

[b]**38** is *N*-[9-chloro-2-(2-furanyl)[1,2,4]triazolo[1,5-c]quinazolin-5-yl]benzene-acetamide. Dataare from Gao and Jacobson.[9]

**Table 3.**

Binding Affinity of a Series of Adenosine Derivatives for Human Wild Type and H95A and W243A Mutant Receptors[a]

| | $K_i$ (nM) | | |
|---|---|---|---|
| | **WT** | **H95A** | **W243A** |
| Adenosine Derivatives | | | |
| **4** | 3.8 ± 0.8 | 85 ± 34 | 6.0 ± 1.3 |
| **5** | 1.9 ± 0.2 | 132 ± 26 | 2.4 ± 0.3 |
| **6** | 142 ± 23 | 615 ± 154 | 137 ± 24 |
| **7** | 114±17 | 796 ± 113 | 100 ± 9 |
| **11** | 1.6 ± 0.2 | ND | 0.9 ± 0.1 |
| **12** [b] | 2.3 ± 0.6 | 60 ± 15 | 2.9 ± 0.5 |
| **15** | 83 ± 9 | ND | 46 ± 19 |
| **1** | 0.8 ± 0.2 | ND | 0.9 ± 0.1 |
| **17** | 3.9 ± 0.4 | 99 ± 17 | 2.7 ± 0.2 |
| **18** | 1.7 ± 0.1 | 460 ± 95 | 1.3 ± 0.1 |
| **19** | 2.1 ± 0.3 | ND | 1.2 ± 0.4 |
| **20** [b] | 1.4 ± 0.4 | 143 ± 36 | 2.1 ± 0.6 |
| **21** | 584 ± 130 | ND | 490 ± 107 |
| Nonnucleoside Antagonists[c] | | | |
| **39** | 238 ± 39 | ND | 2150 ± 230 |
| **40** | 78 ± 11 | ND | 818 ± 97 |

[a] ND, not determined. [$^{125}$I]I-AB-MECA, 1 nM. Protein concentration (10–20 $\mu$g of protein).

[b] Values from ref 29.

[c] **39** is 5-propyl-2-ethyl-4-propyl-3-(ethylsulfanylcarbonyl)-6-phenylpyridine-5-carboxylate; **40** is *S*-1,4-dihydro-2-methyl-6-phenyl-4-(phenylethynyl)-3,5-pyridinedicarboxylic acid, 3-ethyl 5-(phenylmethyl) ester.[61]

**Table 4.**

Binding Affinity of Adenosine Derivatives for Endogenous Rat $A_3$ Receptors Expressed on RBL-2H3 Basophilic Cells and Recombinant Rat $A_3$ Receptors Stably Transfected in CHO Cells[a]

| | $K_i$ (nM) | | | | | |
|---|---|---|---|---|---|---|
| | **5** | **12** | **14** | **18** | **38** | **39** |
| CHO | 1.6 ± 0.3 | 0.9 ± 0.2 | 49 ± 7 | 1.3 ± 0.1 | > 10 $\mu$M | 234 ± 36 |
| RBL-2H3 | 2.7 ± 1.2 | ND | 51 ± 17 | 2.9 ± 0.8 | ND | 357 ± 114 |

[a] [$^{125}$I]4-amino-3-iodobenzyl)adenosine-5′-*N*-methyluronamide (1 nM) was used as a radioligand to determine the binding affinity. ND, not determined. The $K_i$ values ($\mu$M) for **14** at rat brain ARs, measured as described:[6] 12.1 ± 2.4 ($A_1$) and 20.8 ± 0.4 ($A_{2A}$), indicating selectivities of 250- and 420-fold, respectively.